ANALYSIS OF PLASTIC DEFORMATION CHARACTERISTICS DURING METAL CUTTING BY FINITE ELEMENT METHOD

by

SHACHINDRA KUMAR PURWAR

DEPARTMENT OF MECHANICAL ENGINEERING

INDIAN INSTITUTE OF TECHNOLOGY KANPUR

MARCH, 1987

ANALYSIS OF PLASTIC DEFORMATION CHARACTERISTICS DURING METAL CUTTING BY FINITE ELEMENT METHOD

A Thesis Submitted

In Partial Fulfilment of the Requirements

for the Degree of

MASTER OF TECHNOLOGY

by

SHACHINDRA KUMAR PURWAR

to the

DEPARTMENT OF MECHANICAL ENGINEERING

INDIAN INSTITUTE OF TECHNOLOGY KANPUR

MARCH, 1987

ME-1987-M-PUR-ANA

DEDICATED

TO MY

REVEREND PARENTS

CERTIFICATE

18/3/87.

Certified that this thesis work entitled "Analysis of Plastic Deformation Characteristics during Metal Cutting by Finite Element Method" submitted by Shri Shachindra Kumar Purwar in partial fulfilment of the requirements for the degree of Master of Technology of Indian Institute of Technology, Kanpur is a record of bonafide research work carried out by him under our supervision and guidance. The work embodied in this thesis has not been submitted elsewhere for a degree.

(Dr. V.K. JAIN)
Assistant Professor
Dept. of Mechanical Engineering
I.I.T. Kanpur

(Dr.T. SUNDARARAJAN)
Assistant Professor
Dept. of Mechanical Engineeri
I.I.T. Kanpur

18 March, 1987

ACKNOWLEDGEMENT

I express my deep sense of gratitude to Dr. T. Sundararajan for suggesting the problem and supervising the work. I am deeply indebted to him for his inspiring guidance, meticulous attention, constructive criticism and above all for his untiring devotion throughout the tenure of this work.

I am grateful to Dr. V.K. Jain for his invaluable advice and suggestions.

Thanks are due to my friends, Dikshit, Rana, Deshpande, Kannan and Pachauri for their help during this work and make my stay a memorable one.

I am also thankful to my brother and my sisters for their encouragement for higher education.

At the end I am thankful to all those who helped me directly or indirectly during my stay at I.I.T. Kanpur.

SK Purwar

(Shachindra Kumar Purwar)

18 March, 1987

CONTENTS

LIST OF TABLES

LIST OF FIGURES

NOMENCLATURE

$\underline{\underline{d}}$	deviatoric stress
$\underline{\underline{\dot{\varepsilon}}}$	strain rate (per sec.)
$\dot{\bar{\varepsilon}}$	Strain invariant (per sec.)
$\dot{\bar{\varepsilon}}^*$	Dimensional strain invariant
G	modulus of Regidity (N/m^2)
p	mean normal stress (N/m)
t	uncut chip thickness mm
tc	chip thickness (mm)
u	velocity in x direction(m/s)
v	velocity in y direction (m/s)
u^*	dimensionless velocity in x direction (u/v)
v^*	dimensionless velocity in y direction (v/v)
x	horizontal component (m)
y	vertical component (m)
X^*	dimensionless horizontal component (x/t)
γ^*	dimensionless vertical component (y/t)
α	rake angle(degree)
ϕ	shear angle (Degree)
μ	viscosity ($N\text{-}s/m^2$)
ρ	density (kg/m^3)
Ψ	stream function (m^2/s)
ω	vorticity (s^{-1})
σy	Uniaxial yield stress (N/m^2)
λ	Penalty function parametre (m^2/N)
η	natural coordinate

SUPERSCRIPT

e	Element
ne	nodes at an element

SYNOPSIS

An application of FEM technique to estimate the machining zone (or primary shear deformation zone) dimensions in orthogonal metal cutting has been carried out. In this study, metal undergoing plastic deformation is treated as a non-Newtonian, incompressible fluid. The analysis involves the prediction of strain invariant computed using the velocity distribution in the cutting zone using fluid flow equations of mass balance and momentum balance. For the sake of simplicity, it is assumed that the cutting zone is isothermal and no temperature effects on the properties of work material are included. The non-linear fluid flow governing equations are solved iteratively using the FEM procedure based on the Galerkin's approach. The applicability of the model is confirmed by comparing the present results with the available experimental data from earlier studies. It is established that a cut off value of 5 % of the maximum strain rate invariant can be used for approximately demarcating the shear zone.

CHAPTER -I

INTRODUCTION

1.1 GENERAL BACKGROUND :

Metal cutting forms the basis of the modern engineering industry and nearly 40 % of all the engineering products produced every year involve metal cutting directly or indirectly. A basic knowledge of metal cutting process will be helpful in solving various problems encountered during machining in a scientific way. Further, a detailed study of the stresses acting during machining could lead to the prediction of cutting forces and the total power input required for a certain rate of metal removal. The understanding thus gained can help in increasing the productivity and lowering the machining cost and also in the development of new tool materials. Although a large volume of the experimental data about forces and stresses in metal cutting is available. There are not many theoritical models which can accurately predict these variables in metal cutting.

The mechanics of metal cutting is usually studied in terms of the formation of chip. The chip formation mechanism involves the intense plastic deformation of the metal at stresses exceeding the yield stress value at high strain rates. It strongly depends upon several parametres such as the cutting

speed, initial workpiece temperature, the type and geometry of the tool in addition to the basic metallurgical properties of the workpiece material. Experimental observations show that the chip is formed by the shearing of metal in zone known as the shear zone. In the chip formation process, the friction on the tool chip interface also plays an important role. In the present study, some of these aspects of chip formation have been investigated in detail. The deformation process within the shear zone where the chip is formed are analysed with the help of a viscoplastic deformation model.

1.2 REVIEW OF PREVIOUS WORK :

Many investigators have contributed to the theoritical and experimental investigations in metal cutting processes. A pioneering work in the theoritical modelling of metal cutting, is the classical single shear plane model of Merchant and Piispanen [1,2]. According to this model, the formation of the chip is assumed to take place due to the plastic flow along a single plane (known as the shear plane). Average flow stress and slip velocity along the shear plane are obtained through simple geomatric constructions.

The Merchant -Piispanen model has been extended by Palmer and Oxley [3] and Okushima and Hitomi [4] as a thick shear zone model. In zone model, it is assumed that the shear zone is bounded by two parallel planes and the state of stress within the shear zone is Simple Shear. In view of the small thick-

ness of the shear zone (compared to its length), the shear stress is taken to be uniform within the zone.

The first serious attempt to measure the stress and strain properties at high strain rates during machining, appear to have been made by Kececioglu [5] who used a quick stop devic to obtain photo micrographs of the plastic zone in which the chip was formed when machining SAE 1015 steel. From the photo micrographs, the size and shape of the plastic deformation zone estimated by noting the boundaries, where the deformation of grains started and ended . From these results, Kececioglu showed that the plastic zone could be approximately represented by a parallel-sided shear zone.

Further, Stevenson and Oxley [6] used an explosive quick-stop device in conjunction with printed-grids to observe the streamlines of metal flow during machining. Assuming a parallel-sided shear zone model and calculating the strain and strain rates from the stream line observations. They evaluated the values of flow stress as a function of strain for a range of strain rates.

The theoritical prediction of plastic deformation zone in metal cutting based on dislocation mechanics has been presented by Black [7]. He explains the features of the primary deformation zone based on the well-known Cottrell-Stoke

law, wherein the flow stress is partitioned into two parts, a non-thermal part which occurs in the shear fronts (or shear bands) and a thermal part which occur in the lamella regions. He has also investigated the dislocation distribution which either exists in the metal prior to cutting or is produced by the compressive stress field in front of the cutting edge.

Von-Turkovich and others [8,9] have proposed a model of metal cutting in which they argue that the extreme localization of the plastic strains within a small volume a head of the tool edge implies a peculiar form of the plastic flow. According to these authors, the material flows in a viscous manner within the shear zones and behaves like a solid (with infinite viscosity and zero strain rate) outside the shear-zone. However, no numerical solutions of the flow plastic during metal cutting have been obtained in these works.

The flow approach using viscoplastic material behaviour was also employed by Bishop [10] who developed a numerical method to compute the temperature distribution associated with a plane extrusion problem. The same approach has been further extended by Zienkiewicz et al. [11] and Metirano [12] who used a finite element iterative procedure for the modelling of metal forming and extrusion problems. The following steps were adopted by the authors [11,12] in their solution procedure.

(a) Solve the flow problem for a given temperature distribution.

(b) Solve the thermal equation to obtain the temperatures, with a known flow field.

(c) Iterate the flow solution with the plasticity values adjusted according to the temperature field.

At present, there are no FEM studies of the metal-cutting process using the viscoplastic flow approach.

1.3 OBJECTIVES AND SCOPE OF THE PRESENT STUDY :

In the present study, the visco-plastic flow approach proposed by the earlier authors [8-12] is employed for investigating the metal cutting problem. For the sake of simplicity, the thermal effects (which, are in fact quite important for evaluating the material properties) are not considered and properties are evaluated at a typical average temperature of the cutting zone. The plastic flow of the metal is modelled as a highly viscous, non-Newtonian flow with viscosi values strongly depending upon the strain rates. Considering the plastic deformation processes to be dominant in the shear zone and assuming incompressible, pure shear deformation, the resulti flow equations are solved with the help of the Finite Element procedure.

The objectives of the present work are to determine the strain rates in the cutting zone and to establish a theoritical model for the plastic deformation processes which compares favourably with the known experimental results. It is also desired to predict the shape and size of shear deformation zones, based on suitable criteria with regard to the boundaries.

CHAPTER-II

FLOW MODEL FOR METAL CUTTING

A two dimensional orthogonal machining under dry cutting conditions in considered as shown in Fig. (2.1). The tool is assumed to be perfectly sharp with no built up edge (BUE). The work material is taken to be ductile resulting in the formation of a continuous chip. The tool material on the other hand is taken to be perfectly rigid without any deformation. In the present work, metal cutting is assumed to be steady and isothermal. A flow stress model based on the plastic behaviour of the work material is developed here to investigate the various features of the metal cutting process.

2.1 Mechanics of cutting and chip formation :

The metal cutting process can be analysed by stuctying the formation of chip in detail. As uncut metal approaches the tool, it is severely compressed in a region in front of the cutting tool. This causes plastic flow of the metal accompanied by high temperature if the metal is ductile. When the stress in workpiece ahead of the cutting tool reaches a value exceeding the ultimate strength of the metal, the particles shear to form the chip which moves up along the rake face of the tool. The outward or shearing movement of each successive element is

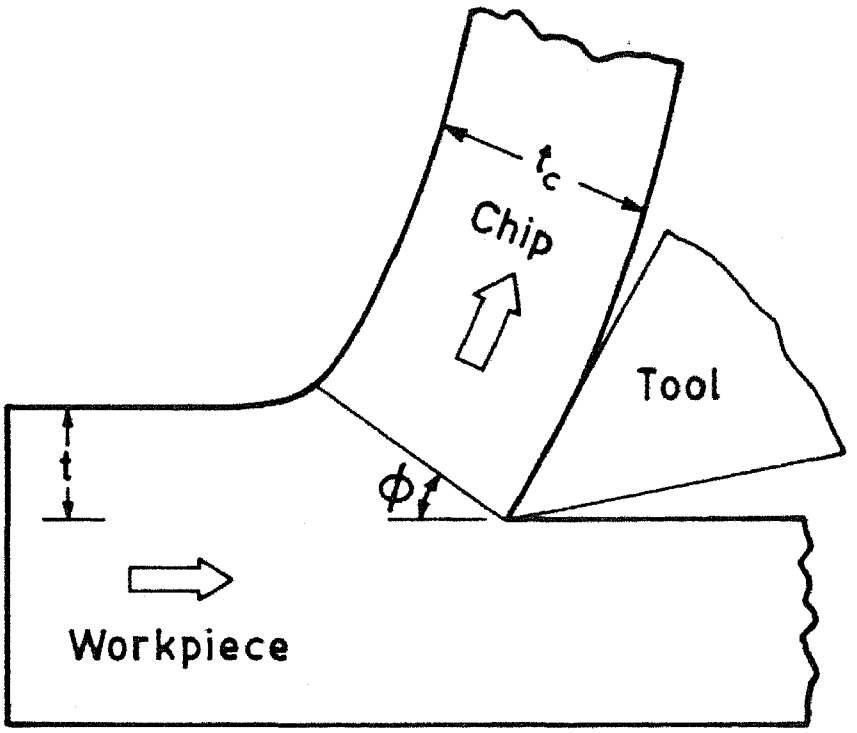

Fig. 2.1. Geometry of Chip Formation in Orthogonal Cutting.

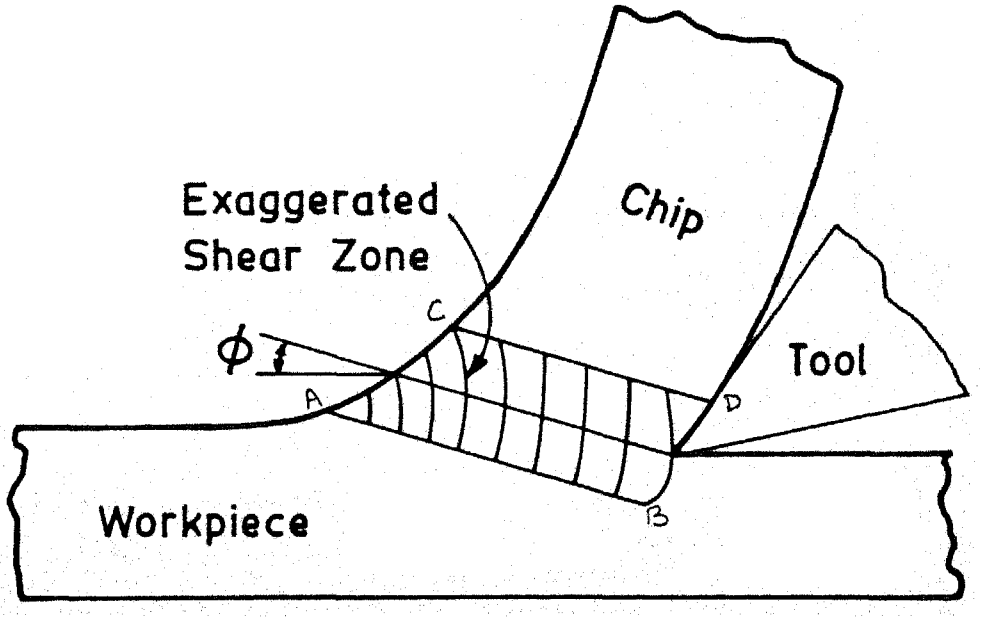

Fig. 2.2. Shear Zone During Metal Cutting.

arrested by work hardening and the movement is transferred to the next element. This process repeats and a continuous type of chip is formed, having a highly compressed and burnished underside and minutely serrated top side caused by the shearing action. The plane along which the elements shear is called the shear plane.

The deformation does not occur sharply across the shear plane, rather it occurs in a narrow band, Metallographic studies (5) have shown that the grains of chip material begin to elongate along the line AB below the shear plane.and continue to do so until they are completely deformed along the line CD, above the shear plane as shown in Fig. (2.2). The region between the lower surface AB, and the upper surface CD is called the shear zone. It has been noted [37] that the shear zone itself consists of two subregions, one in which the metal shears parallel to the shear plane and another in which shearing takes place parallel to the tool surface.

Thus the zone in which plastic flow takes place parallel to the shear zone is known as the primary shear deformation zone (PSDZ) . The primary zone has been observed to be wedge-shaped, and its thickness depends upon machining parameters such as cutting velocity. For instance, it has been reported that an increase in the cutting velocity causes the shear zone thickness to reduce [13]. Plastic deformation of the metal occurs not only in the primary zone, but also in a region close to the tool-chip interference. As the chip moves over the

toolface, a very thin layer of chip which is in contact with the rake face of the tool undergoes additional plastic deformation. This phenomenon is called as secondary shearing and the zone in which secondary shearing occurs is known as Secondary Shear Deformation (SSDZ) Zone . In the secondary zone, each successive layer of metal moves at a different velocity because of the plastic flow. The machined surface below the flank face of tool also undergoes a certain deformation. This happens because of the elastic after effects of the machined surface and flank wear of the tool lead to the high friction between the machined surface and tool flank. Thus, modelling of the chip formation process requires a thorough understanding of the various plastic and elastic deformation of the work material around the cutting edge.

2.2 Theory of Plastic Flow :

Metals deform elastically only in a certain range of small strain. When a metal is strained beyond its elastic limit, it starts yielding and some permanent (plastic) deformation takes place. If the metal is ductile, it undergoes a considerable amount of plastic deformation due to yielding until fracture occurs eventually. The behaviour of plastically deforming materials is rather complicated and fully rigorous. Accurate theories of such behaviour of material are not yet available.

Among plastic solids, an ideal plastic obeying the Von-Mises yielding criterion gives a reasonable abstraction of the behaviour of certain real metals yielding plastically. Here, we shall briefly describe the basic constituents of the plastic flow theory of Von Mises and adopt it for the modelling of the metal cutting problem.

Let us define the stress deviation σ_{ij} and the strain deviations e_{ij} at a point as :

$$\sigma'_{ij} = \sigma_{ij} - \frac{1}{3}\sigma_{ii} \qquad (2.1(a)$$

and

$$e'_{ij} = e_{ij} - \frac{1}{3} e_{ii} \qquad (2.1.a)$$

Where σ_{ij}, e_{ij} are respectively the components of the stress and strain tensors and $\frac{1}{3}\sigma_{ii}$, $\frac{1}{3} e_{ii}$ are respectively the mean values of the normal stress and normal strain. If the material is isotropic and obeys Hooke's law upto the elastic limit, then,

$$e'_{ij} = \frac{1}{2G}\ \sigma'_{ij} \qquad (2.2)$$

where G is the modulus of rigidity. Beyond the elastic limit, e_{ij} is no longer given by the Hooke's law. In this case, we define the plastic strain deviation as the actual strain minus the strain deviation that would be computed if the Hooke's law is still applied. Let the plastic strain deviation be denoted by $e^{(p)}_{ij}$.

$$e_{ij}^{(p)} = e'_{ij} - \frac{1}{2G}\ \sigma'_{ij} \qquad (2.3)$$

The total strain deviation may be written as :

$$e'_{ij} = e_{ij}^{(p)} + \frac{1}{2G}\ \sigma'_{ij} \qquad (2.4)$$

If at each instant of time, the rate of plastic deformation is $\dot{e}_{ij}^{(p)}$, then the increment of plastic strain in the time-interval dt is $\dot{e}_{ij}^{(p)}dt$ and the total plastic deviation after successful stages of yielding will be the algebraic sum of deformation that occurs at all stages.

$$e_{ij}^{(p)} = e_{ij}^{(p)}(0) + \int_0^t \dot{e}_{ij}^{(p)}(t)\ dt \qquad (2.5)$$

where $e_{ij}^{(p)}(0)$ is the initial value of $e_{ij}^{(p)}$ at time t=0

The following assumptions are invoked in the modelling of a Von-Mises type ideal plastic solid.

(i) Hooke's law holds for the mean stress and mean strain at all times.

$$\sigma_{ii} = 3K\ e_{ii} \qquad (2.6)$$

Hence, the plastic strain is incompressible ($e_{ii}^{(p)}=0$) and the plastic strain deviation tensor is same as plastic strain tensor. This justifies the notation $e_{ij}^{(p)}$ in places where normally we would write $e_{ij}^{(p)}$ to indicate a strain deviation.

(ii) The material is elastic and obeys Hooke's as long as the second in variant J_2 is less than a constant K^2. Inother words, no plastic deformation can occur as long as:

$$J_2 = \frac{1}{2} \sigma'_{ij} \sigma'_{ij} < K^2 \qquad (2.7.a)$$

and $$\overset{(p)}{e}_{ij} = 0 \quad \text{when } J_2 < K^2 \qquad (2.7.b)$$

(iii) Yielding can occur (elastic limit is reached) only when $J_2 = K^2$. When the yielding condition $J_2 - K^2 = 0$ prevails, the rate of change of plastic strain is proportional to the stress deviation

$$\dot{e}^{(p)}_{ij} = \frac{1}{\mu} \sigma_{ij} \qquad (2.8)$$

where, μ is positive factor of proportionality which has the dimensions of coefficient of viscosity of fluid.

(iv) Any stress state corresponding to $J_2 < K^2$ can not be realized in the material.

The set of assumptions mentioned above contain two essential parts, namely the criteria for yielding and the stress-strain relationship in the elastic and plastic regions. The yielding condition is based on the second invariant of the stress deviation tensor. Such a yielding criterian was first proposed by Von-Mises. The constant K can be identified with the yield stress in simple shear.

We notice that since only the rate of plastic strain is specified by the above equations for a varying loading sequence, successive plastic increments must be added together algeberically. Such a theory is called an Incremental Theory. Since the material behaves like a viscous fluid when it is in the plastic state, it is called an ideal viscoplastic material.

In many applications of theory of plasticity, the rate at which a plastic flow occurs is of little interest. Sometimes an engineer is concerned only with the total amount of plastic flow. For such application, we often replace equation by the increment law -

$$e_{ij}^{(p)} = \lambda \sigma'_{ij} \qquad (2.9)$$

Where λ is a constant factor of proportionality and not a characteristic constant of material. The sign of λ is determined by the fact that plastic flow involves dissipation of energy under a given set of loading conditions, the value of λ and hence the total plastic flow is determined by the total work done by the external flow.

2.3 Behaviour of Plastic Material :

In large deformation process such as machining involving plastic or Viscoplastic flow, the elastic deformation can be considered as negligible. For such problems, we find that the constitutive relation can be expressed in an Eulerian form

linking the stresses and current strain rates. The situation is thus identical with that of a flow of viscous, non-Newtonian, incompressible fluid Fig. 2.3 gives a partial classification of substances based on their rheological (i.e. shear stress Vs rate of strain) behaviour.

As seen from the fig. non-Newtonian fluids do not follow Newton's law of viscosity (Shear stress = constant x shear strain rate) and the assumption of a constant viscosity independent of temperature, density and shear strain rate does not hold good.

Certain fluids, known as Bingham plastic fluids, behave as a rigid solid until a certain level of shear stress is attained and behave like Newtonian fluids afterwards, as shown in Fig. [2.3]. A general plastic material will have a non-linear variation of shear stress with shear strain rate beyond a critical stress value (yield stress).

2.4 Flow Stress Modelling :

In this study, we shall model the metal undergoing plastic deformation as a non-Newtonian, incompressible fluid (no density change) on the basis of the discussions presented in articles 2.2 and 2.3.

For such a viscous and incompressible fluid, we can write the constitutive relationship in the form

$$\sigma_{ij} = -p\delta_{ij} + 2\mu \dot{e}_{ij}, \quad \delta_{ij} = 1 \quad i=j \qquad (2.10)$$
$$= 0 \quad i \neq j$$

where $(-p)$ is the mean normal stress and $\dot{e}_{ij}$ is the strain rates.

The strain rate components in two dimensions can be written (Eqn.(2.11)) in terms of only the first (linear) order components of the deformation rate tensor, neglecting the higher order velocity derivatives.

$$\dot{e}_{11} = \frac{\partial u}{\partial x} \; ; \; \dot{e}_{12} = \dot{e}_{21} = \frac{1}{2}\left(\frac{\partial u}{\partial x} + \frac{\partial u}{\partial x}\right); \; \dot{e}_{22} = \frac{\partial v}{\partial y} \qquad (2.11)$$

where u and v are the velocity components in x and y directions, respectively. Rewrite the strain rate tensor as :

$$\dot{e}_{ij} = \frac{1}{2\mu} d_{ij} \qquad (2.12)$$

in which d_{ij} are the deviatoric components of stress.

In the present work, for a Von-Mises type of plastic material modelled as an isotropic, in compressible, non-Newtonian fluid, the variation in viscosity is given by (14)

$$\mu = \frac{\sigma_y + \left(\dot{\bar{e}}/\gamma \sqrt{3} \right)^{1/n}}{\sqrt{3}\ \dot{\bar{e}}} \qquad (2.13)$$

In the above equation, μ is the non-linear viscosity, γ and n are the physical constants determining the visco-plastic behaviour of the material and σ_y is the uniaxial yield stress

of the material which is in general a function of temperature, pressure and deviatric strain invariant $\dot{\bar{e}}$. The strain in variant can be represented in terms of the velocity derivatives as follows :

$$\dot{\bar{e}} = \sqrt{2\ \dot{e}_{ij}\ \dot{e}_{ij}}$$

$$= \sqrt{2\ (\dot{e}_{11}^2 + \dot{e}_{22}^2 + 2\dot{e}_{12}\ \dot{e}_{21})}$$

$$= \sqrt{2\left\{\left(\frac{\partial u}{\partial x}\right)^2 + \frac{1}{2}\left(\frac{\partial u}{\partial y} + \frac{\partial v}{\partial x}\right)^2 + \left(\frac{\partial v}{\partial y}\right)^2\right\}} \qquad (2.14)$$

2.5 Governing Equations :

For steady orthogonal metal cutting operation with the width of cut much larger than the feed or depth of cut, a two dimensional model may be employed. Treating the model as a non-Newtonian, incompressible fluid in the machining zone, the governing equations are given by :

$$\underline{\nabla}\ .\underline{V} = 0. \qquad \text{(mess balance for incompressible fluid)} \qquad (2.15)$$

$$\rho\ \underline{V}.\ \underline{\nabla}\ \underline{V} = \nabla.\ \underline{\underline{\sigma}} \qquad \text{(Momentum balance)} \qquad (2.16)$$

In the above equation stress tensor can be written as :

$$\underline{\underline{\sigma}} = -p\ \underline{\underline{I}} + \underline{\underline{d}} = -p\ \underline{\underline{I}} + \mu\ (\underline{\nabla}\ \underline{V} + \underline{V}\ \underline{V}^T) - 2/3\ \mu\ (\underline{\nabla}.\underline{V})\ \underline{\underline{I}} \qquad (2.17)$$

where p is the pressure and $\underline{\underline{d}}$ is the deviatoric stress tensor. Using equation (2.17) in equation (2.16)

$$\rho \underline{V}.\underline{\nabla}\underline{V} = -\underline{\nabla} p + \underline{\nabla}.\left(\mu \left\{\underline{\nabla}\underline{V} + \underline{V}\underline{\nabla}^{T}\right\}\right) \qquad (2.18)$$

In component form, from eqn.(2.18) we can write x and y momentum equation as

X-momentum

$$\rho\left(u\frac{\partial u}{\partial x} + v\frac{\partial u}{\partial y}\right) = -\frac{\partial p}{\partial x} + \frac{\partial}{\partial x}\left(2\mu\frac{\partial u}{\partial x}\right) + \frac{\partial}{\partial y}\left\{\mu\left(\frac{\partial u}{\partial y} + \frac{\partial v}{\partial x}\right)\right\} \qquad (2.19.a)$$

Y-momentum

$$\rho\left(u\frac{\partial v}{\partial x} + v\frac{\partial v}{\partial y}\right) = -\frac{\partial p}{\partial y} + \frac{\partial}{\partial x}\left\{\mu\left(\frac{\partial u}{\partial y} + \frac{\partial v}{\partial x}\right)\right\} + \frac{\partial}{\partial y}\left(2\mu\frac{\partial v}{\partial y}\right) \qquad (2.19.b)$$

The mass balance equation (2.15) can be rewritten as :

$$\frac{\partial u}{\partial x} + \frac{\partial v}{\partial y} = 0 \qquad (2.19.c)$$

2.6 Boundary Conditions :

The boundary conditions for solving equations (2.19.a,b,c) are basically of two types. Or surfaces I, II, III, V and VI (Fig. 2.4), the velocity components are specified. On surfaces IV and VII zero traction and zero normal velocity are specified. In mathematical form, we have

(i) $u = V$ (cutting velocity)

$v = 0$ on surfaces I, II, III (2.20.a)

(ii) $u = V_c \sin\alpha$

$v = V_c \cos\alpha$ on surface VI (2.20.b)

where V_c is chip velocity and α is the rake angle.

(iii) For surfaces IV and VII

$$v_n = 0$$

$$\underline{n} \cdot \underline{g} = 0 \qquad (2.20.c)$$

where v_n and $\underline{n}$ are normal velocity and the unit normal vector respectively at a point on the surface.

(iv) On surface V, upto a length h, the slip velocity at the interface between the chip and the tool is presented. From the experimental measurements of Tay et.al. [D4]

$$V_s \doteq \frac{1}{3} V_c \sqrt{1 + 8s/h}$$

Where V_c is the chip velocity and s is the distance from the cutting edge measured along the interface. Beyond the plastic contact length h, the velocity is taken to be equal to the chip velocity on the surface V. Therefore,

$$u = \frac{1}{3} V_c \sqrt{1 + 8s/h} \sin\alpha$$

$$v = \frac{1}{3} V_c \sqrt{1 + 8s/h} \cos\alpha \qquad \text{for } s \leq h \qquad (2.20.d)$$

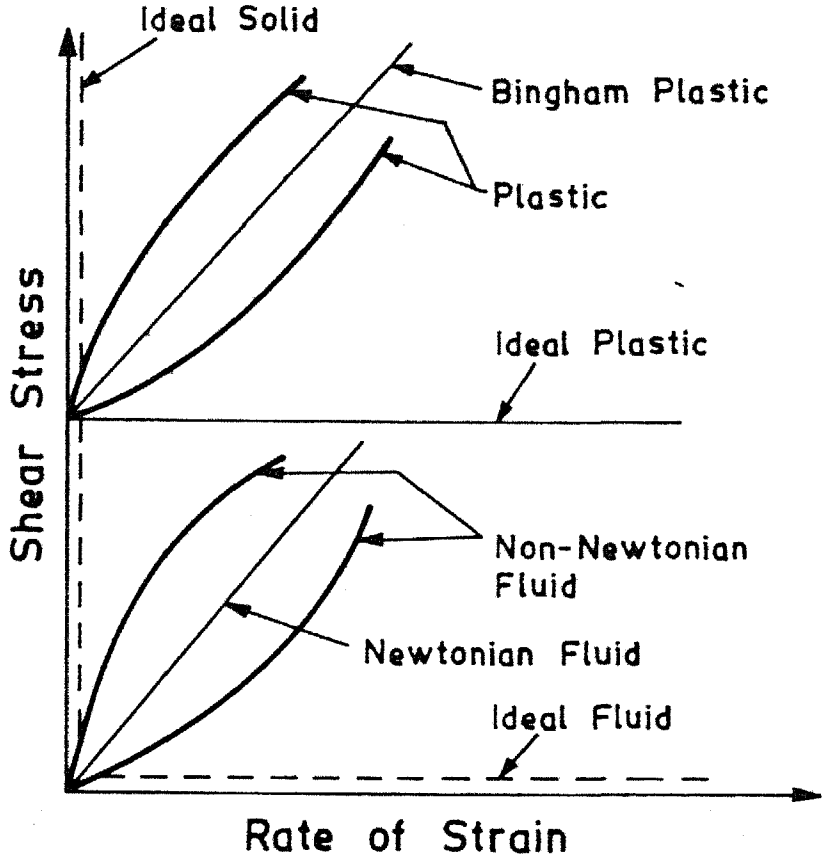

Fig. 2.3. Rhelogical Classification of Flow.

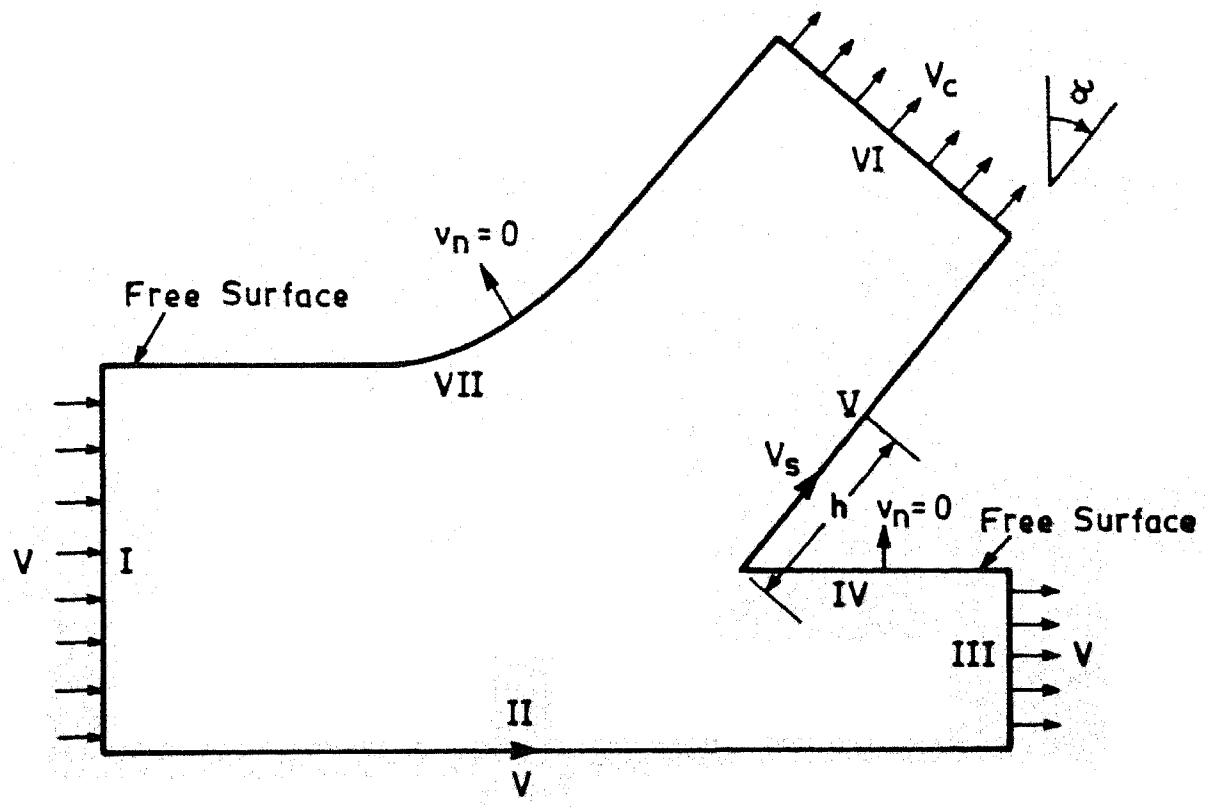

Fig. 2.4. Problem Regions, Showing the Boundry Conditions.

$$u = V_c \sin\alpha$$
$$v = V_c \cos\alpha \qquad \text{for } s > h \qquad (2.20.e)$$

2.7 Non-Dimensionalization :

Writing the Eons. [2.13(a,b,c)] in a dimensionaless form facilitates generalisation to model a large range of problem. In this respect, following dimensionless variables can be used

$$x^* = x/t \quad , \quad y^* = y/t$$
$$u^* = u/V \quad , \quad v^* = v/V$$

where V is the cutting velocity and t is the thickness of uncut chip.

Now, the dimensionless form of the continuity equation will be

$$\frac{\partial u^*}{\partial x^*} + \frac{\partial v^*}{\partial y^*} = 0 \qquad (2.21.a)$$

writing the dimensionless form of the x-momentum of equation.

$$\frac{\rho V^2}{t}\left(u^* \frac{\partial u^*}{\partial x^*} + v^* \frac{\partial u^*}{\partial y^*}\right) = -\frac{1}{t}\frac{\partial p}{\partial x^*} + \frac{V}{t^2}\left[\frac{\partial}{\partial x^*}\left(2\mu \frac{\partial u^*}{\partial x^*}\right) + \frac{\partial}{\partial y^*}\left\{\mu\left(\frac{\partial u^*}{\partial y^*} + \frac{\partial v^*}{\partial x^*}\right)\right\}\right]$$

Let $p^* = p/\sigma_y$, $\mu^* = \mu/\left(\frac{\sigma_y t}{V}\right)$ and $\sigma^* = \sigma_y/\rho V^2$

where σ_y is the uniaxial yield stress.

On simplifying,

$$\frac{1}{\sigma^*}\left(u^*\frac{\partial u^*}{\partial x^*}+v^*\frac{\partial u^*}{\partial y^*}\right) = -\frac{\partial p^*}{\partial x^*}+\frac{\partial}{\partial x^*}\left(2\mu^*\frac{\partial u^*}{\partial x^*}\right)+\frac{\partial}{\partial y^*}\left\{\mu^*\left(\frac{\partial u^*}{\partial y^*}+\frac{\partial v^*}{\partial x^*}\right)\right\} \qquad (2.21.b)$$

Similarly the y-momentum equation can be put in dimensionless form as :

$$\frac{1}{\sigma^*}\left(u^*\frac{\partial v^*}{\partial x^*}+v^*\frac{\partial v^*}{\partial y^*}\right) = -\frac{\partial p^*}{\partial y^*}+\frac{\partial}{\partial x^*}\left\{\mu^*\left(\frac{\partial u^*}{\partial y^*}+\frac{\partial v^*}{\partial x^*}\right)\right\}+\frac{\partial}{\partial y^*}\left(2\mu^*\frac{\partial v^*}{\partial y^*}\right) \qquad (2.21.c)$$

From Eqn. (2.13). The normalized variation of viscosity is given by

$$\mu^* = \mu/\sigma_y t/V = \frac{1+B^*(\dot{e}^*)^{1/n}}{\sqrt{3}\,\dot{e}^*} \qquad (2.22)$$

where $B^* = \frac{1}{\sigma_y}\left(\frac{V}{\sqrt{3}t^{\gamma}}\right)^{1/n}$

The boundary condition can also be easily non-dimensionalized as shown above. All velocities in Fig. (2.4) are scaled by V and lengths are scaled by t, to obtain the dimensionless boundary conditions.

CHAPTER- III

FINITE ELEMENT ANALYSIS

3.1 INTRODUCTION :

The solution procedure that has been adopted for the problem under study is the Finite Element Method. Some of most important advantages of the FEM procedure are the easy handling of a complex geomatrical shape of the solution domain and the general manner in which boundary conditions can be introduced. Rather than requiring every trial solution to satisfy the boundary conditions, the condition may be presented after obtaining the algebraic equations for assemblage. Since the boundary conditions do not enter into the equations for the individual finite elements, one can use the same field variable model for both internal and boundary elements. Morover, the field variable models need not be changed, when the boundary conditions change. In addition to the easy accomodation of complex geometry and boundary conditions, the FEM technique has also been successful in representing complicated material property variation that are difficult to incorporate into other numerical methods for example, formulations in solid mechanics have been devised for anistropic, non-linear, time dependent or temperature dependent material

behaviour. In the present problem, the geometry is complicated and a strong non-linearity is present due to the high variation of viscosity in the plastic flow region. Therefore, the FEM procedure is quite suitable for obtaining the velocity field solutions.

3.2 DESCRIPTION OF FEM TECHNIQUE :

In FEM, the governing differential equations are converted into an equivalent set of integeral equations which are minimized in some sense over the whole solution domain. The solution domain is divided into several small elements of known shape and the solution variable is approximated within each of these elements by suitable approximating functions. The integeral governing equations are then evaluated within each element using the approximating functions and all such elemental integrals are assembled to obtain the final matrix equation to be solved. The above steps can be summed up as follows :

(a) Obtain the equivalent integral equations for describing the problem. The boundary conditions of the problem would be transformed into appropriate boundary integrals.

(b) Divide the solution domain into several elements and place chosen number of nodes within each element. Obtain the approximating functions for describing the field variable, within each element in terms of the nodal values.

$$L(\phi^*) = R \qquad (3.2)$$

Where, R is the residue which may be a function of the spatial coordinates and time. In Galerkin's procedure, the residue, weighted appropriately by suitable weighting functions, is minimized over the whole solution domain D in an integral sense. In mathematical form, this becomes :

$$\int_D W_i \, R \, dv = \int_D W_i \, L(\phi^*) dv = 0, \text{ for each } i \qquad (3.3)$$

where, W_i are the weighting functions. The approximation ϕ^* may be written as a piece continuous profile for each element as:

$$\phi^{*(e)} = \sum_{i=1}^{m} N_i^{(e)} \, \phi_i^{(e)} \qquad (3.4)$$

In the above equation, m is the number of nodes per element and $N_i^{(e)}$ are the approximating functions for representing ϕ^* within the element (e) which are called as the Shape Functions of the element (e). The nodal values of ϕ^* for the element (e) are denoted by $\phi_i^{(e)}$. In Galerkin's procedure, the weighting function W_i are taken to be the same as the shape functions $N_i^{(e)}$ within each element.

3.3 TYPES OF FORMULATION :

There are four types of formulation which are in use for obtaining the finite solution of any flow problem. These are :

(i) STREAM FUNCTION FORMULATION

(ii) STREAM FUNCTION AND VORTICITY FORMULATION

(iii) VELOCITY PRESSURE FORMULATION

(iv) PENALITY FUNCTION FORMULATION

The stream function approach for solving a flow problem was first proposed by OSLON [16]. By introducing the stream function Ψ, the continuity equation can be satisfied exactly and the momentum equation can be combined into a single function in terms of Ψ. The main disadvantage of this formulation is that the governing equation is a fourth order differential equation and interpolation functions of high order are required. Also in order to obtain velocity and pressure, further processing of results is required.

In the stream function vorticity formulation, in stead of dealing with a single governing equation fourth order, the stream function (Ψ) and vorticity (w) are chosen as the unknowns and two governing equations of second order in Ψ and w result [17]. In this formulation, the boundary conditions may consist of specified values of Ψ and w or specified values of their first derivatives. The principal difficulty in using the stream function-vorticity formulation is that, in general, vorticity is unknown a priori along solid boundaries.

In the velocity pressure formulation, the pressure and velocity components are considered as the nodal variables. This formulation isused because of the following advantages :

(1) The formulation is readily extended to three dimensions.

(2) Only C^o (linear element) continuity is required of the element interpolation functions.

(3) Pressure, velocity, velocity gradient and stress boundary conditions can be directly incorporated into the matrix equations :

(4) Free surface problems are tractable.

(5) The formulation requires less computational time than stream function and vorticity formulation (17).

The penality function approach [18] is very popular procedure in which the pressure variable is eliminated and only the velocity components are solved. In the present study, we shall use this approach because retaining pressure as a variable often leads to numerical difficulties. The penality formulation involves treating continuity equation as a constraint among the velocity components and the continuity constraints is introduced into the momentum equation in a Lagrange multiplier λ, It is possible to choose λ to be very large and eliminate the pressure in terms of λ. The boundary condition to be specified for this formulation are either specified values of velocity components or specified values of their first derivatives.

3.4 DERIVATION OF FINITE ELEMENT EQUATIONS :

The dimensionless governing equations (after dropping the stars for convenience) are :

$$\frac{1}{\sigma}\left(u\frac{\partial u}{\partial x}+v\frac{\partial u}{\partial y}\right)=-\frac{\partial p}{\partial x}+\frac{\partial}{\partial x}\left(2\mu\frac{\partial u}{\partial x}\right)+\frac{\partial}{\partial y}\left\{\mu\left(\frac{\partial u}{\partial y}+\frac{\partial v}{\partial x}\right)\right\} \qquad (3.5.a)$$

$$\frac{1}{\sigma}\left(u\frac{\partial v}{\partial x}+v\frac{\partial v}{\partial y}\right)=\frac{-\partial p}{\partial y}+\frac{\partial}{\partial x}\left\{\mu\left(\frac{\partial u}{\partial y}+\frac{\partial v}{\partial x}\right)\right\}+\frac{\partial}{\partial y}\left(2\mu\frac{\partial v}{\partial y}\right) \qquad (3.5.b)$$

$$\frac{\partial u}{\partial x}+\frac{\partial v}{\partial y}=0 \qquad (3.5.c)$$

In the present work, the incompressibility constraint Eqn.(3.5.c) has been treated with the help of a penality function approach. Introducing a parameter λ such that $\lambda >> p$, the in compressibility condition can be approximately written as :

$$\frac{\partial u}{\partial x}+\frac{\partial v}{\partial y}=-p/\lambda \qquad (3.6)$$

Now, using Eqn.(3.6) in Eqns.(3.6.a and b), we obtain :

$$\frac{1}{\sigma}\left(u\frac{\partial u}{\partial x}+v\frac{\partial u}{\partial y}\right)=\lambda\frac{\partial}{\partial x}\left(\frac{\partial u}{\partial x}+\frac{\partial v}{\partial y}\right)+\frac{\partial}{\partial x}\left(2\mu\frac{\partial u}{\partial x}\right)+\frac{\partial}{\partial y}\left\{\mu\left(\frac{\partial u}{\partial y}+\frac{\partial v}{\partial y}\right)\right\} \qquad (3.7.a)$$

$$\frac{1}{\sigma}\left(u\frac{\partial v}{\partial x}+v\frac{\partial v}{\partial y}\right)=\lambda\frac{\partial}{\partial y}\left(\frac{\partial u}{\partial x}+\frac{\partial v}{\partial y}\right)+\frac{\partial}{\partial x}\left\{\mu\left(\frac{\partial u}{\partial y}+\frac{\partial v}{\partial x}\right)\right\}+\frac{\partial}{\partial y}\left(2\mu\frac{\partial v}{\partial y}\right) \qquad (3.7.b.)$$

The unknown u and v in the above equations can now be expanded in terms of nodal values and appropriate interpolation function in the form :

$$u = \sum_{i=1}^{n} N_i^u \, u_i \qquad (3.8.a)$$

$$v = \sum_{i=1}^{n} N_i^v \, v_i \qquad (3.8.b)$$

where, N_i^u and N_i^v are the interpolating functions (which need not necessarily be of the same order) and u_i and v_i are the nodal values of the unknown. Following Yamada et. al [19] in order to simplify the algebraic structure of the equations, we select $N_i^u = N_i^v$. Eight noded isoparametric elements are used for dividing the solution domain. For the isoparametric elements, the global coordinates x,y of apoint within are element may be transformed as :

$$x = \sum_{i=1}^{8} N_i \, x_i \qquad (3.9.a)$$

$$y = \sum_{i=1}^{8} N_i \, y_i \qquad (3.9.b)$$

The velocity shape functions, N_i for the for 8-noded isoparametric element are given in Fig. (3.1) in terms of local coordinate ξ , η by the following formulae :

Corner nodes :

$$N_i = \frac{1}{4} (1+\xi_i \, \xi) \, (\xi_i \, \xi+\eta_i \, \eta-1) \qquad (3.10.a)$$

Midside nodes :

$$N_i = \frac{1}{2}\,(1-\zeta^2)\,(1+\eta_i\,\eta) \qquad (3.10.b)$$

$$N_i = \frac{1}{2}\,(1+\zeta_i\,\zeta)\,(1-\eta^2) \qquad (3.10.c)$$

Employing the Galerkin's weighted residual approach, Equation (3.7.a) becomes.

$$\sum_1^{ne} \int_A e N_i \Big[\frac{1}{\sigma} \Big\{ \sum_1^n N_k \lambda_k \sum_1^n \frac{\partial N_j}{\partial x} u_j + \sum_1^n N_k\, u_k \sum_1^n \frac{\partial N_j}{\partial y} u_j \Big\} -$$

$$\lambda \frac{\partial}{\partial x} \Big(\sum_1^n \frac{\partial N_j}{\partial x} u_j + \sum_1^n \frac{\partial N_j}{\partial y} v_j \Big) - \Big\{ \frac{\partial}{\partial x} \Big(2\mu \sum_1^n \frac{\partial N_j}{\partial x} u_j \Big) + \frac{\partial}{\partial y}$$

$$\Big[\mu \Big(\sum_1^n \frac{\partial N_j}{\partial y} u_j + \sum_1^n \frac{\partial N_j}{\partial x} v_j \Big) \Big) \Big\} \Big] dA^e = 0 \qquad (3.11)$$

Where the outer summation is overall the area elements in the domain end the inner summation is overall the appropriate number of nodes of an element. In the present case, the number of nodes per element, n=8.

Invoking the Green's theorem , the second order terms can be partially integerated as :

$$\int_{A(e)} N_i \Big\{ \lambda \frac{\partial}{\partial x} \Big(\sum_1^n \frac{\partial N_j}{\partial x} u_j + \sum_1^n \frac{\partial N_j}{\partial y} v_j \Big) \Big\}\, dA^e =$$

$$\int_{\gamma e} N_i \Big[\lambda \Big(\frac{\partial u}{\partial x} + \frac{\partial v}{\partial y} \Big) n_x ds - \int_A \Big[\lambda \frac{\partial N_i}{\partial x} \Big(\sum_1^n \frac{\partial N_j}{\partial x} u_j + \sum_1^n \frac{\partial N_j}{\partial y} v_j \Big) \Big] dA^e$$

and

$$\int_{A^e} N_i \left\{ \frac{\partial}{\partial x} \left(2\mu \sum_1^n \frac{\partial N_j}{\partial y} u_j\right) + \frac{\partial}{\partial y}\left[\mu\left(\sum_1^n \frac{\partial N_i}{\partial y} u_j + \sum_1^n \frac{\partial N_j}{\partial x} v_j\right)\right] \right\} dA^e$$

$$= \int_{\gamma e} N_i \left[\left(2\mu \frac{\partial u}{\partial x}\right) n_x + \mu\left(\frac{\partial u}{\partial y} + \frac{\partial v}{\partial x}\right) n_y\right] ds - \left[\int_{A^e} \frac{\partial N_i}{\partial x} .2\mu \sum_1^n \frac{\partial N_j}{\partial x} u_j \right.$$

$$\left. + \frac{\partial N_i}{\partial y} .\mu \left(\sum_1^n \frac{\partial N_j}{\partial y} u_j + \sum_1^n \frac{\partial N_j}{\partial x} v_j\right)\right] dA^e$$

Where γ^e denotes the element surface, when the contribution from two adjacent elements are summed up a shown in Fig. (3.2). The find contribution from the side becomes zero unless it happens to be part of a boundary.

The required form of Equation 3.11 is

$$\sum_1^{ne} \int \left[\frac{1}{\sigma}\left(N_i N_k u_k \frac{\partial N_j}{\partial x} u_j + N_i N_k v_k \frac{\partial N_j}{\partial y} v_j\right) + \frac{\partial N_i}{\partial x} .2\mu \frac{\partial N_j}{\partial x} u_j \right.$$

$$+ \frac{\partial N_i}{\partial y} .\mu \frac{\partial N_j}{\partial y} u_j + \frac{\partial N_i}{\partial y} \mu \frac{\partial N_j}{\partial x} v_j + \left(\frac{\partial N_i}{\partial x} .\lambda \frac{\partial N_j}{\partial x} u_j + \frac{\partial N_i}{\partial x} \lambda \frac{\partial N_j}{\partial y} v_j\right) \Big] dA^e$$

$$- \int_{\gamma e} N_i \left[\left(2\mu \frac{\partial u}{\partial x}\right) n_x + \mu\left(\frac{\partial u}{\partial y} + \frac{\partial v}{\partial x}\right) n_y + \lambda\left(\frac{\partial u}{\partial x} + \frac{\partial v}{\partial y}\right) n_x\right] ds = 0$$

(3.12)

In the above equation, the summation sign Σ has been dropped by adopting the convention that summation is implied if a subscript is repeated in the same form.

Now, the momentum equation in y direction may similarly be written as :

$$\sum_{1}^{ne} \Big[\int_{A^e} -\frac{1}{\sigma}(N_i N_k u_k \frac{\partial N_j}{\partial x} v_j + N_i N_k v_k \frac{\partial N_j}{\partial y} v_j)$$

$$+ \frac{\partial N_i}{\partial x} \mu \frac{\partial N_j}{\partial y} u_j + \frac{\partial N_i}{\partial x} \mu \frac{\partial N_j}{\partial x} v_j + \frac{\partial N_i}{\partial y} 2\mu \frac{\partial N_j}{\partial y} v_j$$

$$+ (\frac{\partial N_i}{\partial y} \lambda \frac{\partial N_j}{\partial x} u_j + \frac{\partial N_i}{\partial y} \lambda \frac{\partial N_j}{\partial y} v_j) \Big] dA^e - \int_{\gamma^e} N_i \Big[\mu(\frac{\partial u}{\partial y} + \frac{\partial v}{\partial x}) n_x +$$

$$(2\mu \frac{\partial v}{\partial y}) n_y + \lambda (\frac{\partial u}{\partial x} + \frac{\partial v}{\partial y}) n_y \Big] ds = C \qquad (3.13)$$

The final assembled form of the above equations (3.12, 3.13) is

$$[A][X] = [B] \qquad (3.14)$$

where, the vector x contrains all the nodal unknown u_i and v_i. It is possible to write the coefficient matrix $[A]$ in the sub-matrices $[c_{ij}]$ as follows :

$$[A] = \sum_{1}^{ne} \int_{A^e} \begin{bmatrix} c_{11} & c_{12} \\ c_{21} & c_{22} \end{bmatrix} dA \qquad (3.15)$$

where

$$C_{11} = (N_i N_k \bar{u}_k \frac{\partial N_j}{\partial x} + N_i N_k \bar{u}_k \frac{\partial N_j}{\partial y}) \frac{1}{\sigma} + \mu \left(2 \frac{\partial N_i}{\partial x} \cdot \frac{\partial N_j}{\partial x} + \frac{\partial N_i}{\partial y} \cdot \frac{\partial N_j}{\partial y}\right) + \lambda \frac{\partial N_i}{\partial x} \cdot \frac{\partial N_j}{\partial x}$$

$$C_{12} = \mu \frac{\partial N_i}{\partial y} \cdot \frac{\partial N_j}{\partial x} + \lambda \frac{\partial N_i}{\partial x} \cdot \frac{\partial N_j}{\partial y} \qquad (3.16.a\text{-}d)$$

$$C_{21} = \mu \frac{\partial N_i}{\partial x} \cdot \frac{\partial N_j}{\partial y} + \lambda \frac{\partial N_i}{\partial y} \cdot \frac{\partial N_j}{\partial x}$$

$$C_{22} = (N_i N_k \bar{u}_k \frac{\partial N_j}{\partial x} + N_i N_k \bar{u}_k \frac{\partial N_j}{\partial y}) \frac{1}{\sigma} + \mu \left(\frac{\partial N_i}{\partial x} \cdot \frac{\partial N_j}{\partial x} + 2 \frac{\partial N_i}{\partial y} \cdot \frac{\partial N_j}{\partial y}\right) + \lambda \frac{\partial N_i}{\partial y} \cdot \frac{\partial N_j}{\partial y}$$

In the above expressions, we have treated $\bar{u}$ and $\bar{v}$ as known values (from previous iteration) for the sake of making the matrix equation (3.14) quasi-linear.

On the boundaries where natural boundary conditions are imposed, these line integerals appear in the right hand side vector as illustrated below : The column vector is written as :

$$b_i = \sum_{1}^{ne} \int_{\gamma^e} \begin{Bmatrix} b_1 \\ b_2 \end{Bmatrix} ds \qquad (3.17)$$

where

$$b_1 = N_i \left[(2\mu \frac{\partial u}{\partial x}) n_x + \mu (\frac{\partial u}{\partial y} + \frac{\partial v}{\partial x}) n_y + \lambda (\frac{\partial u}{\partial x} + \frac{\partial v}{\partial y}) n_x \right]$$

(3.18.a)

$$b_2 = N_i \left[\mu\left(\frac{\partial u}{\partial y} + \frac{\partial v}{\partial x}\right) n_x + \left(2\mu \frac{\partial v}{\partial y}\right) n_y + \lambda \left(\frac{\partial u}{\partial x} + \frac{\partial v}{\partial y}\right) n_y \right]$$

(3.18.b)

The matrix equation (3.14) is non-linear due to the variation of viscosity μ and also due to ineratial terms. Therefore, one needs to employ a suitable iterative procedure for determining the nodal unknowns.

3.5 MATRIX SOLUTION TECHNIQUE :

The solution procedure used here for the solution of the assembled matrix equation is known as the Frontal Method [20]. When the number of unknown in the problem is very large, the method adopted for solving the assembled equation has a significant bearing on the computer storage requirement and execution time. It is very difficult to solve these equations by simple matrix inversion techniques. The Frontal Method is based on direct Gaussian ellimination for solving the symmetric matrices where the leading diagonal is always used as apivot. For unsymmetric metrices, encountered in a wide range of engineering problem, the most suitable pivot is not necessarily on the leading diagonal and frontal solution routine exist for off diagonal pivoting (6). This however tend to be more time consuming. The method used here uses only diagonal pivoting incorporates many features of the Frontal method for solvi symmetric matrices.

In general terms, the overall solution technique consists of :

(1) Formation of Element matrices

(2) Assembling into a Global matrix

(3) Introduction of Boundary Conditions

(4) Reduction of Global fluid matrix using a Gaussian elimination technique.

(5) A back substitution process.

3.6 BASIC PHILOSPHY OF THE FRONTAL METHOD :

The primary objective of the frontal method is the elimination of variables as soon as possible after their introduction, into the global matrix via the appropriate equations. As soon as the contribution from all the elements to a particular nodal point have been assembled, the corresponding variable associated with that node can be eliminated. The complete matrix is therefore never assembled since the reduced equations can be eliminated from core and stored on disc. The equations held in core, with the corresponding nodes and variables are collectively called as the Front and the number of unknown variables in the front is termed as the Front Width. The front width changes continually since only after the contribution to a particular node have been fully summed, the corresponding equation reduction based on a diagonal pivot can be executed.

A preassigned global matrix core area is first filled from contributing elements and then the largest diagonal entry in the preassigned core is found and used as a pivot in a direct Gaussian Elimination process. As the maximum pre-determined number of equations are eliminated the corresponding reduced equations are written on to the disc and more elements and corresponding equations are taken into core. The Fig. [3.3] shows the basic idea of the Frontal Method. The equations, nodes and variables currently in core are termed **Active**, those assigned to disc are **Deactivated** and those yet to appear in core are **Inactive**.

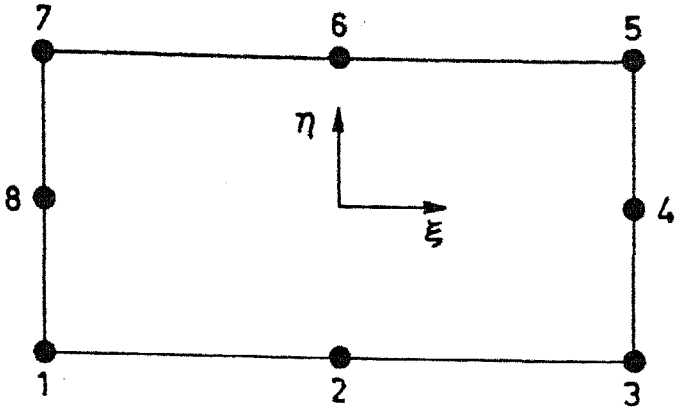

Fig. 3.1. Eight Noded Element Showing the Local Co-ordinate System.

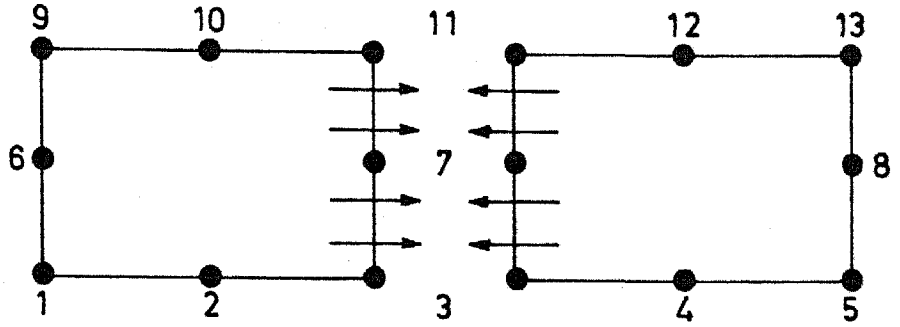

Fig. 3.2. Typical Element Interface Where Residual of Surface Integral ≃ 0.

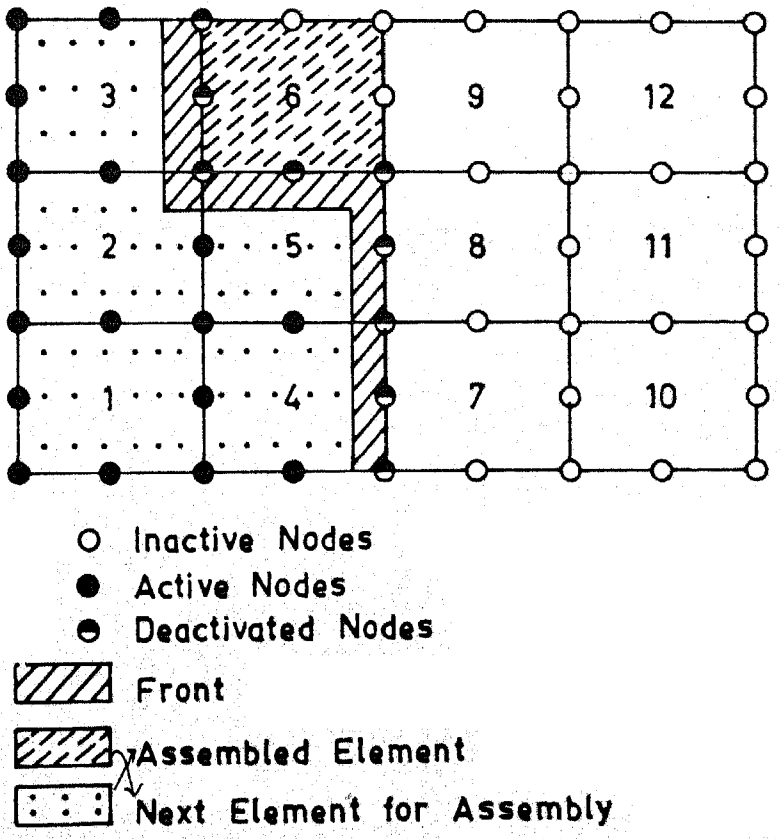

Fig. 3.3. Definitions of Front and Element Numbering for Minimum Front Width.

CHAPTER -IV

RESULTS AND DISCUSSION

Using FEM technique in the viscoplastic model of metal cutting, results are obtained for strain rate invariant, stream lines and mean width of primary shear deformation zone. To test the validity and accuracy of the model, analytical results are compared with experimental results. To test the sensitivity of the model, a parametric study has also been conducted. Results and discussion have been divided into three subheadings.

(i) Mean width of primary shear deformation zone

(ii) Flow lines during metal cutting

(iii)(a) Effect of different parametres on the mean width of PSDZ and $\Delta s/t$.

(b) Distribution of strain rate invariant in PSDZ.

(i) Mean width of Primary shear deformation zone :

In Fig. 4.1-4.3, constant strain rate invariant curves have been plotted for three different cutting conditions. The strain rate invariant ($\dot{\bar{e}}$)has been normalised with respect to its maximum value ($\dot{\bar{e}}_{max}$); for each cutting condition, graphs of normalized isostrain rate invariant ($\dot{\bar{e}}/\dot{\bar{e}}_{max}$) equal to 3 %, 4 % and 5 %. have been plotted.

In order to estimate the size of PSDZ (or mean width of PSDZ), normals extending up to the desired curve say 5 %. cutt off point, are drawn on the shear plane (Fig. 4.1). Then the average of all these normals is calculated and is defined as the mean width of PSDZ (Δs). It is to be noted that secondary shear deformation zone and a part of PSDZ (shaded area for 5 %. curve in Fig. 4.1) is excluded to simplify the measurement procedure. However, better method to determine Δs, could be to divide the total area under the curve by the shear plane length. After comparing the mean width of PSDZ with the experimental results (Table 4.1), it is seen that for all the three cutting conditions, the three percent curve consistently gives the primary shear zone thickness which agrees will with the experimental results. Therefore, it was decided to use the cut-off value of normalized strain rate invariant as three percent in the present analysis for investigating the properties of the shear zone.

The shape of three percent curve indicates that the primary shear zone is approximately Wedge-Shaped and the secondary shear zone adjacent to the rake face is approximately triangular (shadow portion near the tool,chip contact). Also it is seen (Fig. 4.1-4.3) that the plastic deformation zone

TABLE 4.1

Comparision of Experimental (Ref. 6) and Theoritical value of mean width of Primary Shear Deformation zone.

S.No	Cutting Condition				Mean width of PSDZ (s/t)			
	α (Degree)	ϕ Degree	u (m/s)	t(mm) $\times 10^{-4}$	Experimental	cut-off value $\dot{\bar{e}} / \dot{\bar{e}}^*_{max}$ 3%	4%	5%
1	10	25.0	3.07	1.75	0.725	0.743	0.686	0.410
2	10	28.0	2.05	1.05	1.05	1.083	0.820	0.624
3	10	28.0	4.15	0.648	0.648	0.668	0.459	0.382

extends a little below the cutting edge into the machined metal. These predictions are in good accordance with the known results from experiments (Turkovich and Micheletti [21], Okushima and Hitomi [4]).

(ii) Flow Lines during metal cutting :

In Fig. (4.4.a,b), the flow paths of metal particles during metal cutting are presented for two different cutting conditions. It is seen from these plots that the paths of the particles are straight lines in both the uncut metal and fully formed chip, and sharp turning takes place in a thin zone in front of the cutting edge. It is this turning that contributes chiefly to the shear strain rate and the plastic flow of the metal occurs in this zone only. Photographical observations of printed-grids over the workpiece by Stevenson and Oxley [6] have shown that the flow path of metal particles can be approximated by hyperbolic strain lines. The results of the present study are in good agreement with these experimental observations.

(iii)(a) Effect of different parametres on the mean width of PSDZ and $\Delta s/t$:

Having established the validity of theoritical model, a set of hypothetical cutting conditions were considered in order to study the effects of the important cutting parametres such as cutting velocity (v), feed (t) and the shear angle (ϕ)

upon the deformation zone thickness. The effect of the cutting velocity (v) upon the dimensionless shear zone thickness ($\Delta s/t$) in shown in Fig. 4.5. It is seen that $\Delta s/t$ decreases with V. This trend has also been observed experimentally by Nakayoma [22] and Okushima and Hitomi [4]. From the theoritical point of view, the decrease of $\Delta s/t$ with V may be explained as follows. Its extent of the shear deformation zone depends upon the value of viscosity. For a low value of viscosity, a smaller zone is expected and vice-versa. A higher cutting velocity (at const t) results in a higher strain rate, which leads to a lower value of viscosity as seen from equation 2.13. Therefore, at higher speeds, the dimensionless shear zone thickness is smaller.

In fig. 4.6, the effect of the shear angle ϕ upon $\Delta s/t$ is shown. It is seen that $\Delta s/t$ decreases with ϕ. For smaller value of ϕ, chip becomes thicker and so the length of the shear plane in deformation zone increases. However, if the amount of material to be removed and the rate of metal removal are fixed (i.e. fixed value of t and v), the total deformation undergone by the metal is more or less constant. Therefore, while the length of the shear zone increases, due to an increase in ϕ, its thickness reduces. The trend seen in the present result was earlier noted by Pandey and Jain (23).

The effect of the undeformed chip thickness t, upon the mean width of the primary shear zone Δs is shown in Fig. 4.7. The mean width Δs increases approximately in proportion with t,

as was noted by Nakaynama [22]. It appears that angular shape of the shear deformation zone is more or less a constant when all the parametres other than t are constant. Therefore, as increases with t.

(iii)(b) Distribution of Strain invariant in PSDZ :

In Fig. 4.8, the variation of the a dimensionless parameter $[\dot{\bar{e}}^* = (\dot{\bar{e}}/(v/t))]$ is plotted against the other dimensionless parameter [distance ζ /t] measured along the shear plane from the cutting edge. As expected, high strain rate values occur in the vicinity of the cutting edge and far away from the cutting edge, $\dot{\bar{e}}^*$ is smaller. In metal cutting theory, for the sake of simplicity, it is often assumed that the shear stress and rate of the shear strain are constant along the shear plane. The present results show that the strain rate is not constant and that a better assumption be that shear strain varies with ζ (Fig. 4.8).

In Fig. 4.9, the dimensionless parameter $\dot{\bar{e}}^*$ is plotted against the dimensionless distance (η/t) travelled by a particle through the deformation zone. It is found that $\dot{\bar{e}}^*$ decreases on either side of the shear plane as the particle moves away from the shear plane. It is obvious because on one side it is moving towards the uncut work material where $\dot{\bar{e}}^*$ is approximately zero: On the other side, it is moving towards the fully formed chip where no further deformation takes place, hence $\dot{\bar{e}}^*$ would again attain a zero value.

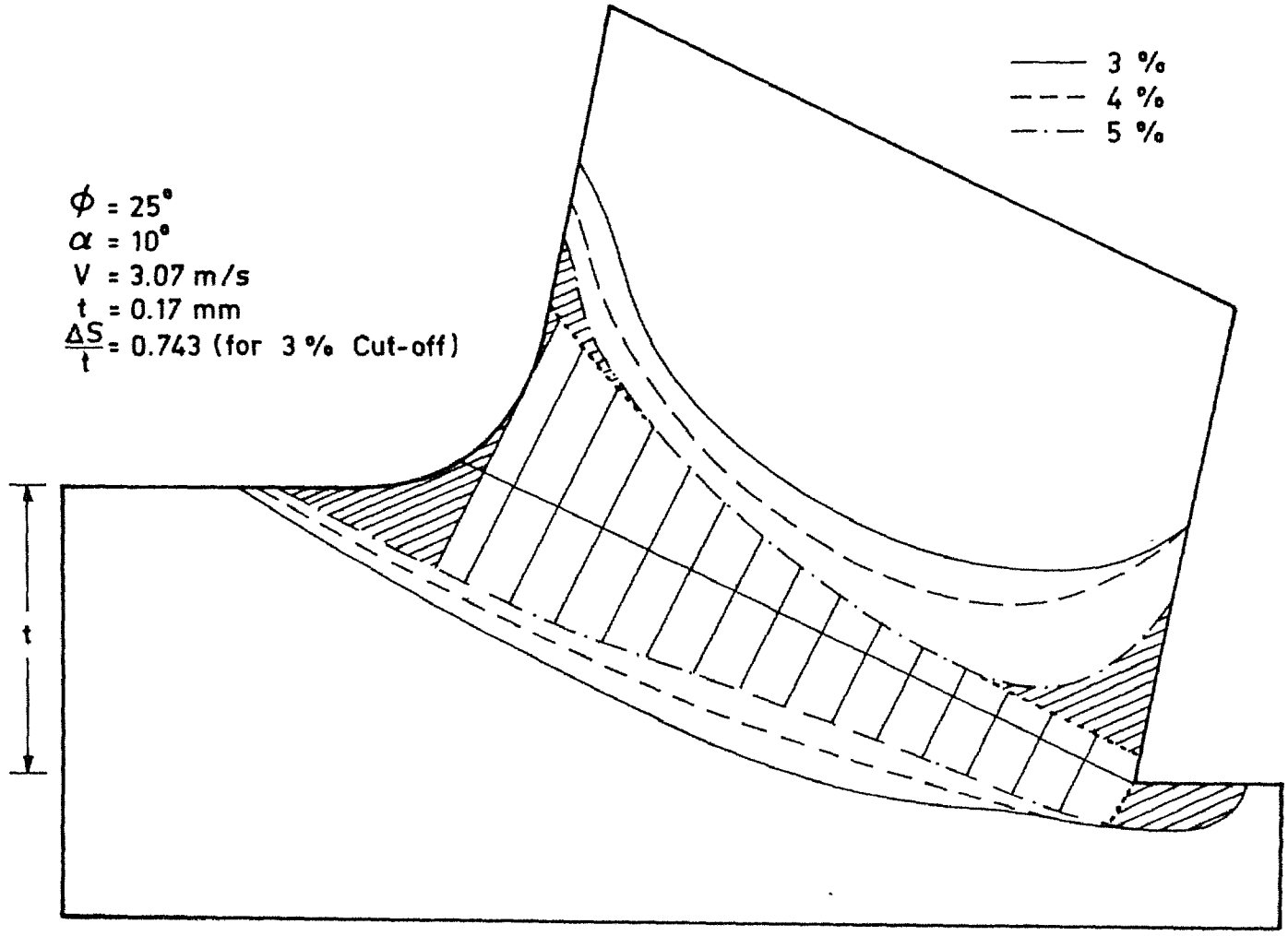

Fig. 4.1. Constant Strain Rate Curves During Metal Cutting.

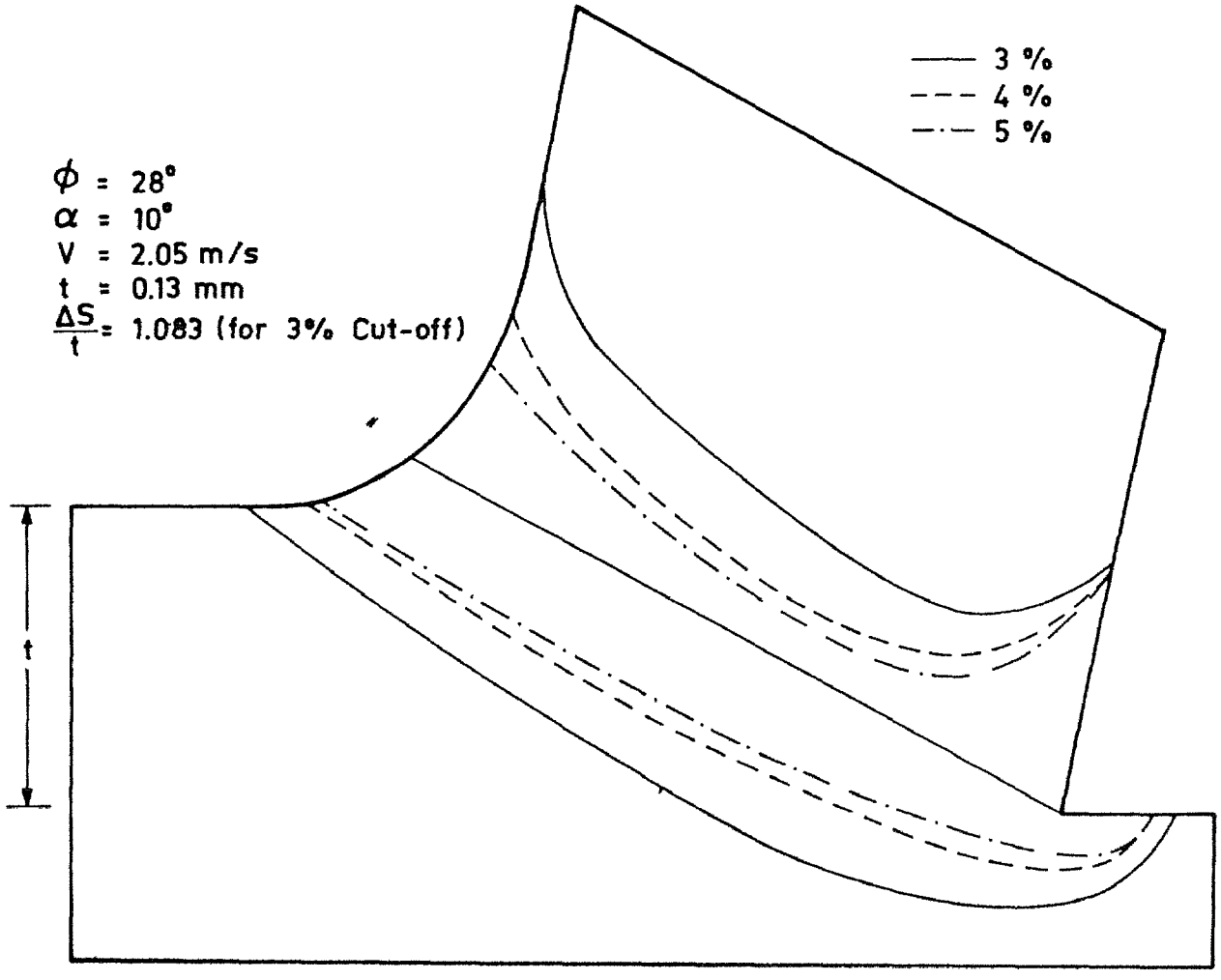

Fig. 4.2. Constant Strain Rate Curves During Metal Cutting.

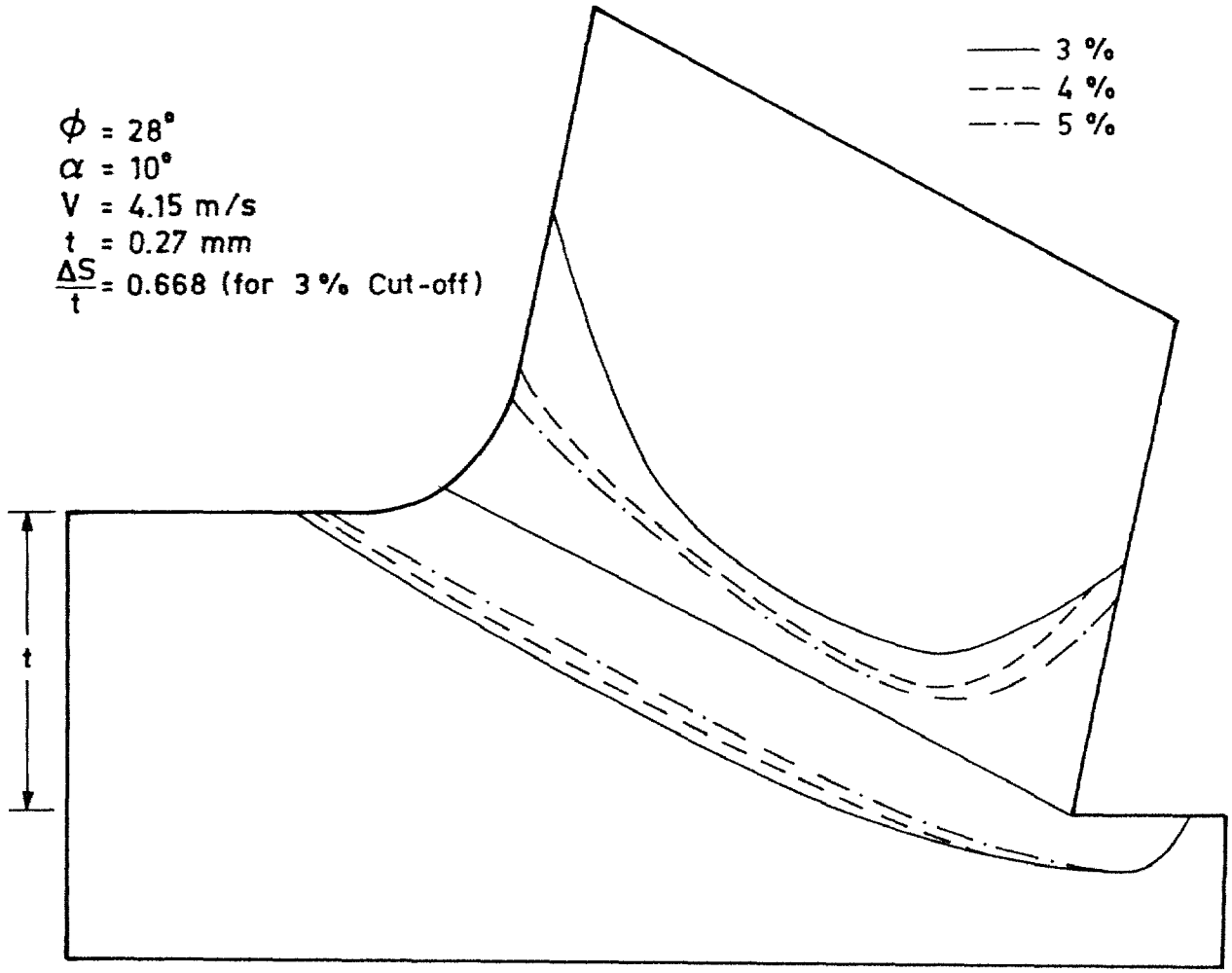

Fig. 4.3. Constant Strain Rate Curves During Metal Cutting.

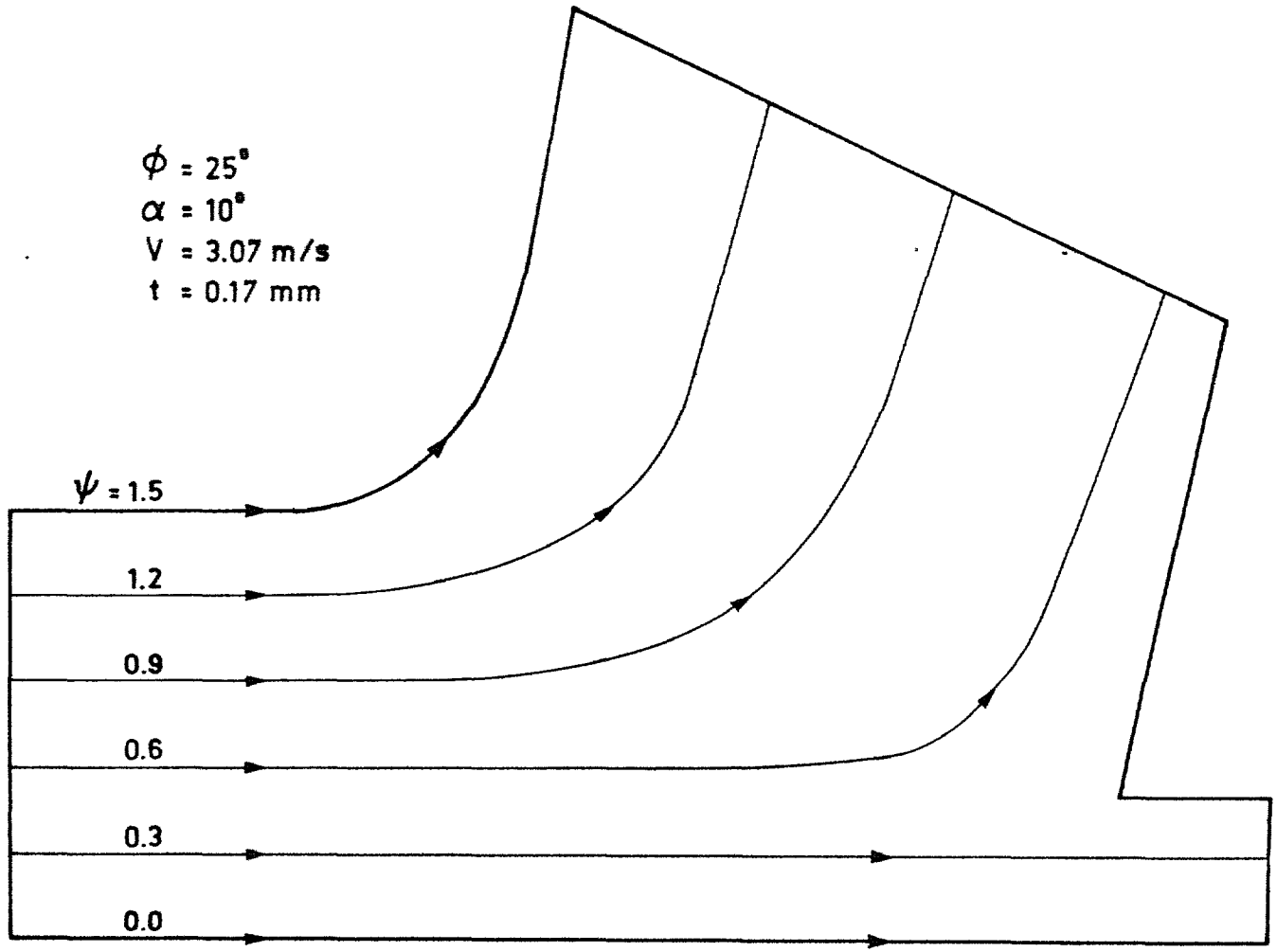

Fig. 4.4a. Flow Lines During Metal Cutting.

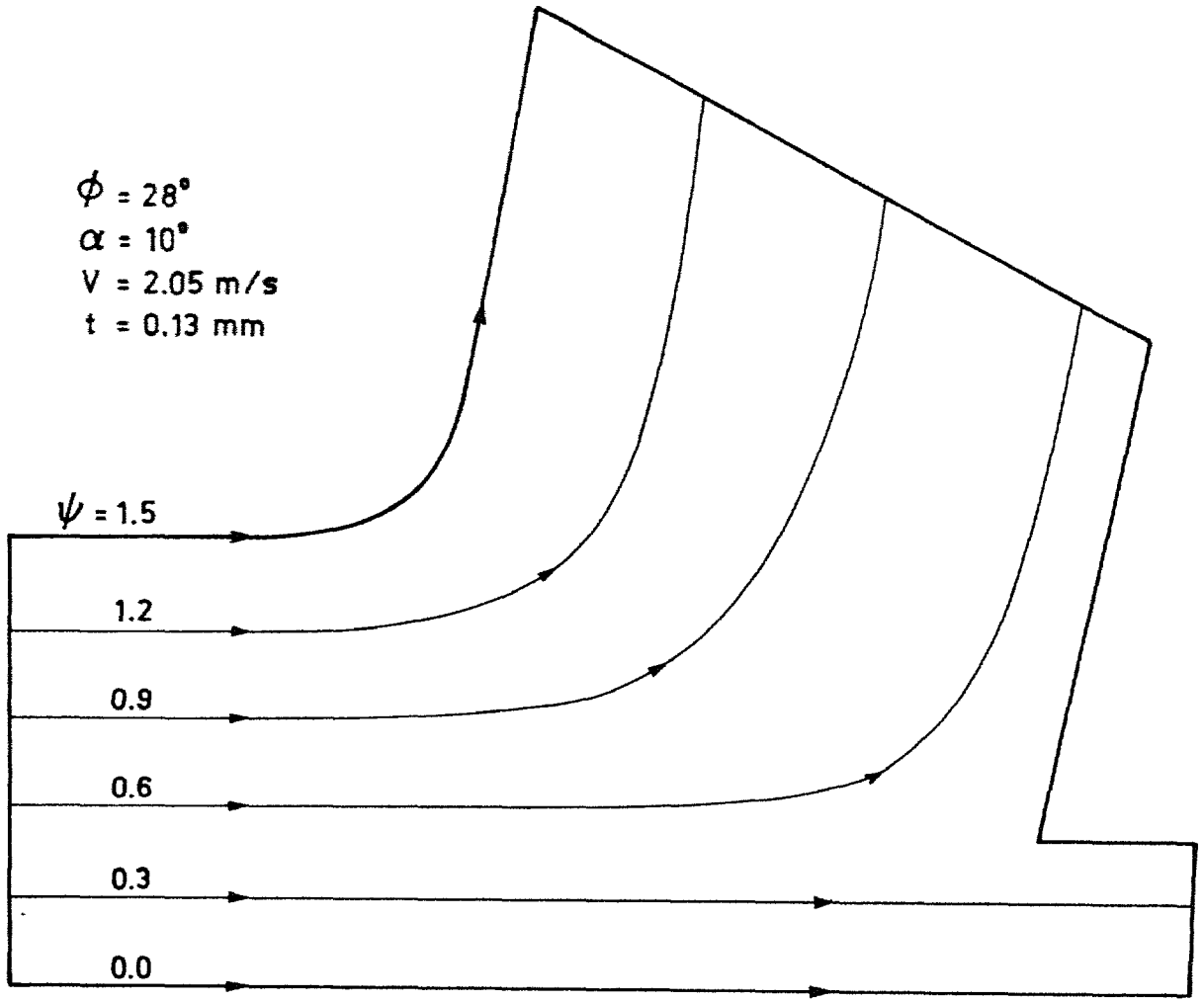

Fig. 4.4b. Flow Lines During Metal Cutting.

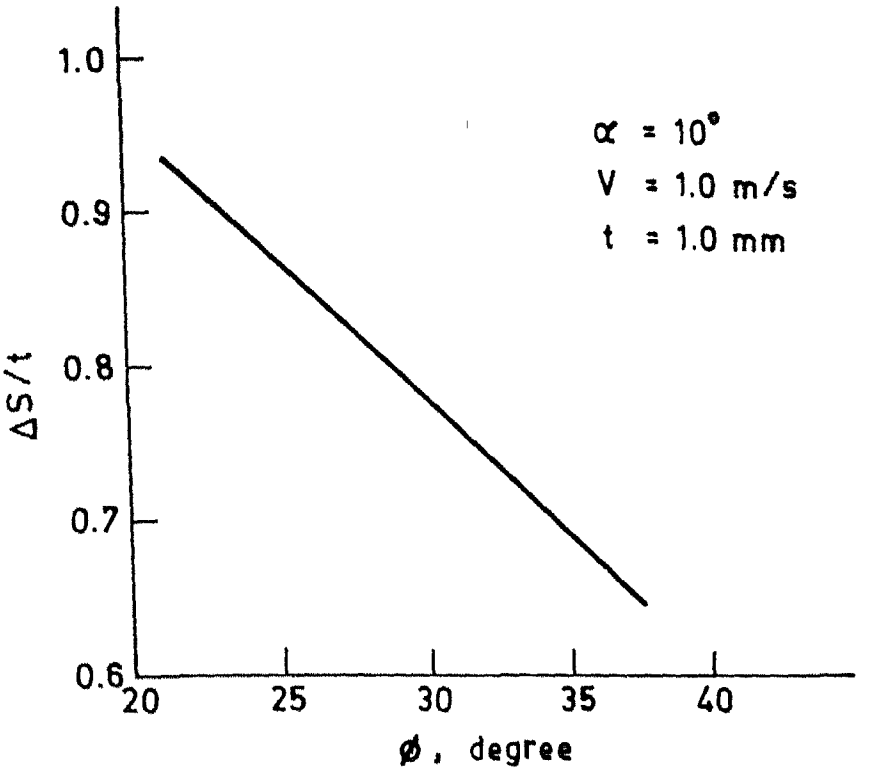

Fig. 4.6. Effect of Shear Angle on Dimensionless Mean Width of Primary Shear Deformation Zone.

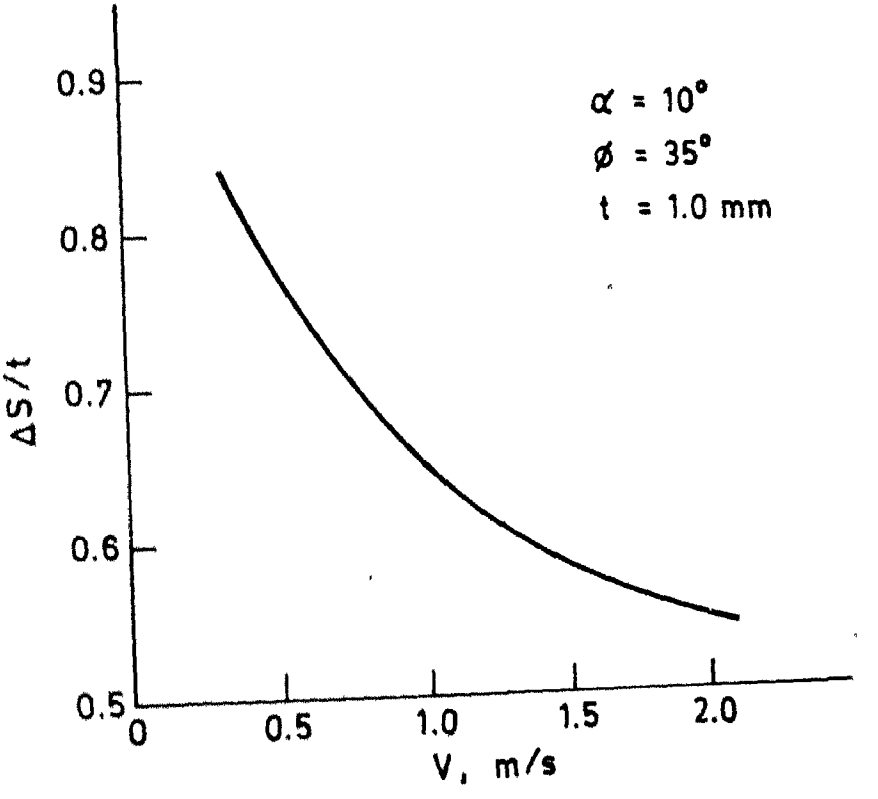

Fig. 4.5. Effect of Cutting Velocity on the Dimensionless Mean Width of Primary Shear Deformation Zone.

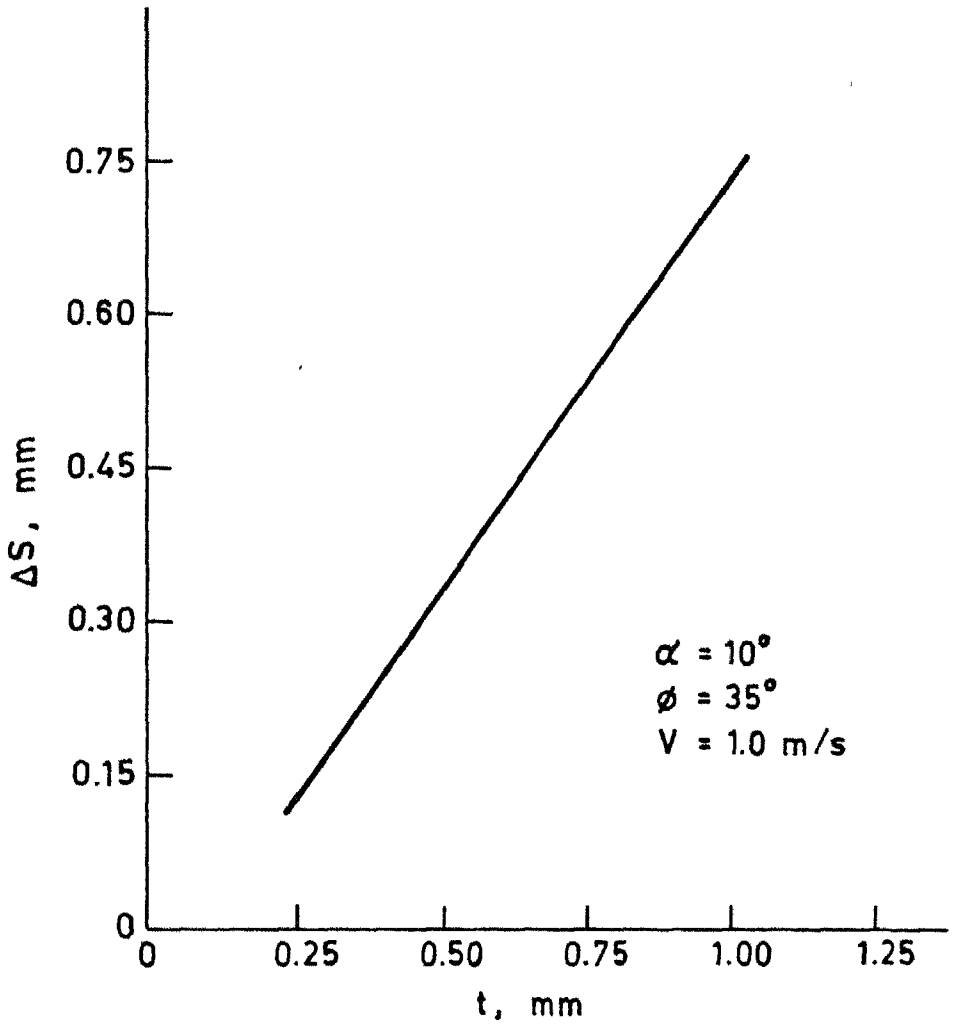

Fig. 4.7. Effect of Undeformed Chip Thickness on Mean Width of Primary Shear Deformation Zone.

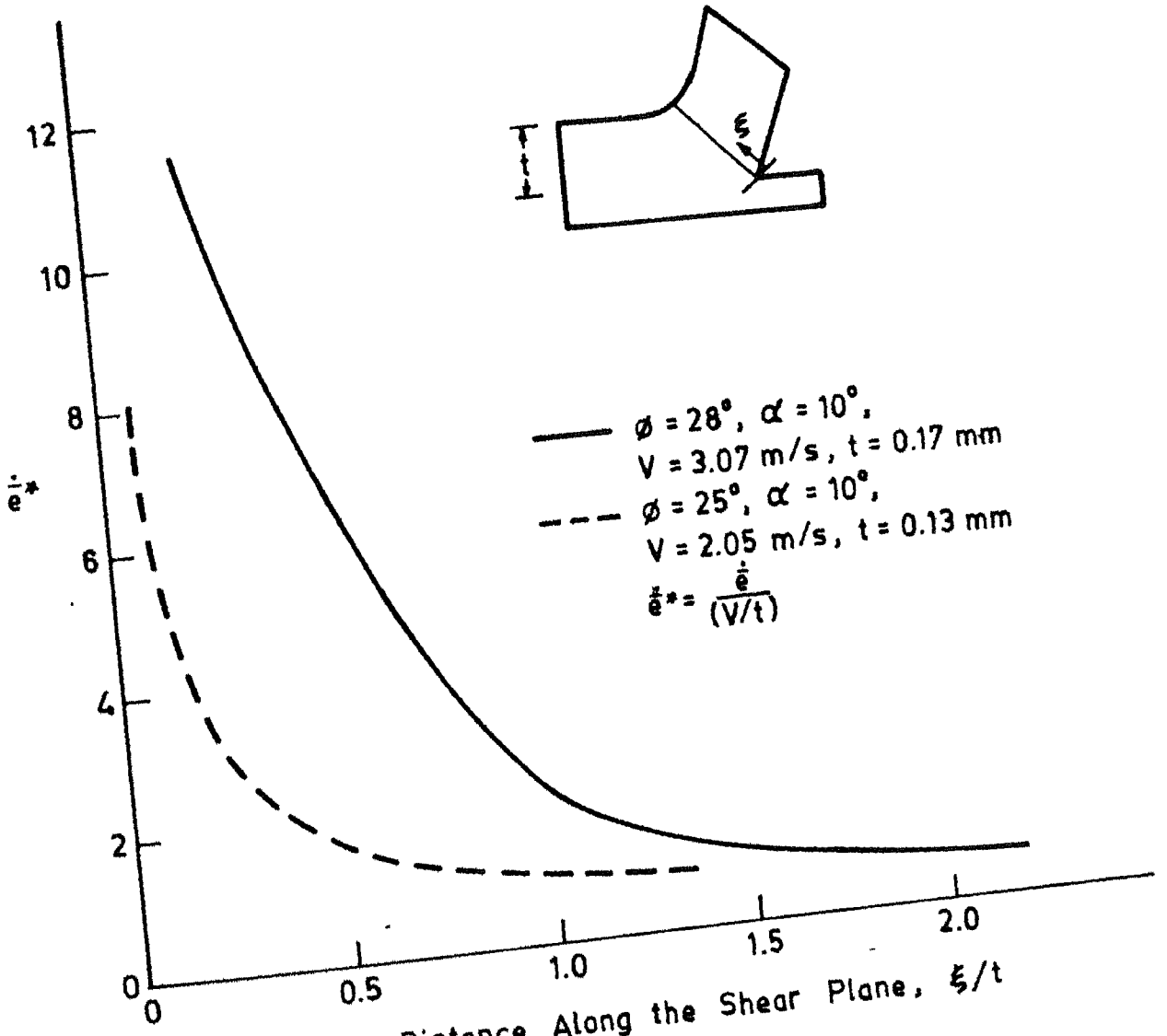

Fig. 4.8. Variation of Dimensionless Strain Rate Along the Shear Plane.

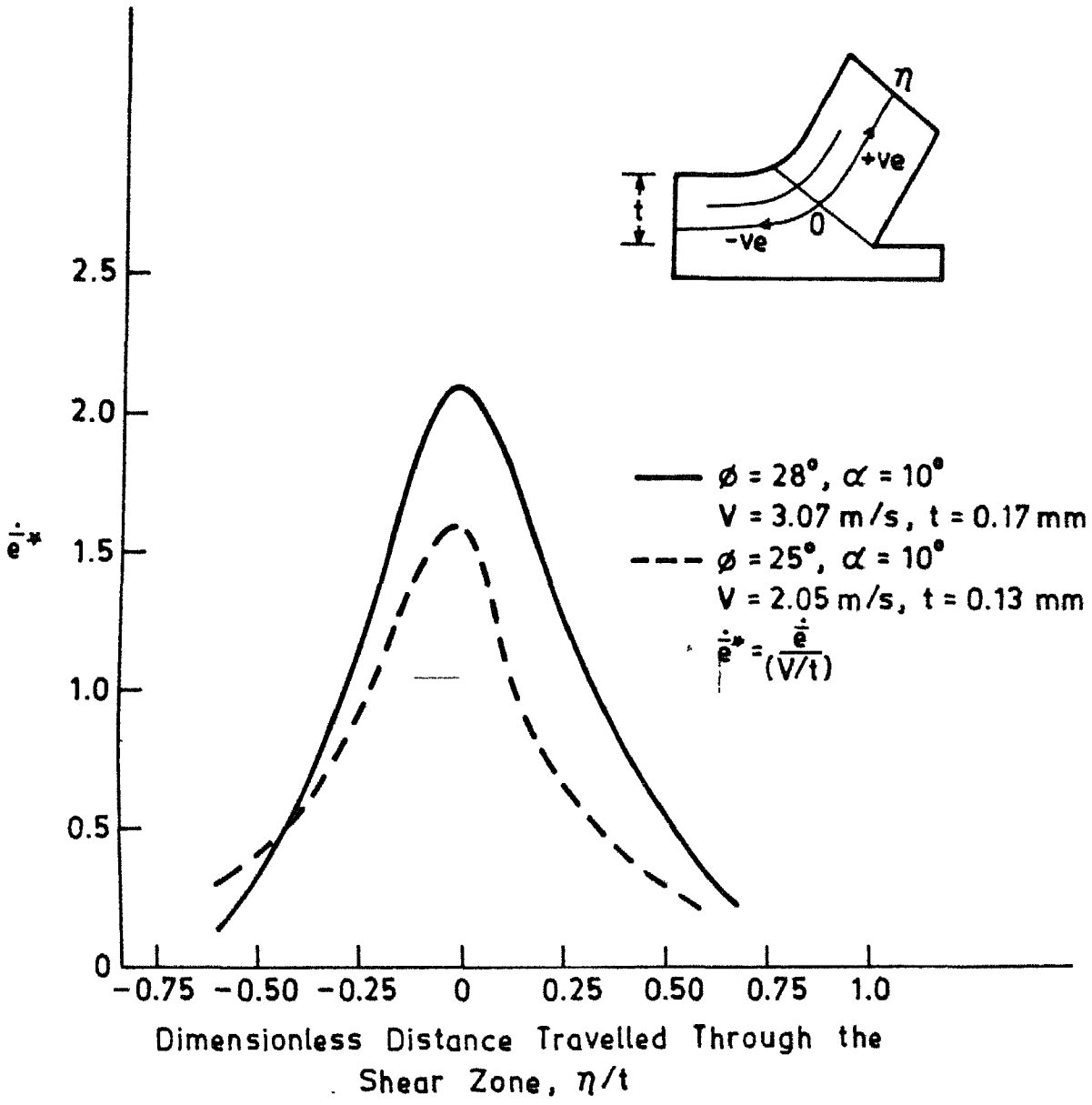

Fig. 4.9. Variation of Dimensionless Strain Rate Across the Shear Zone.

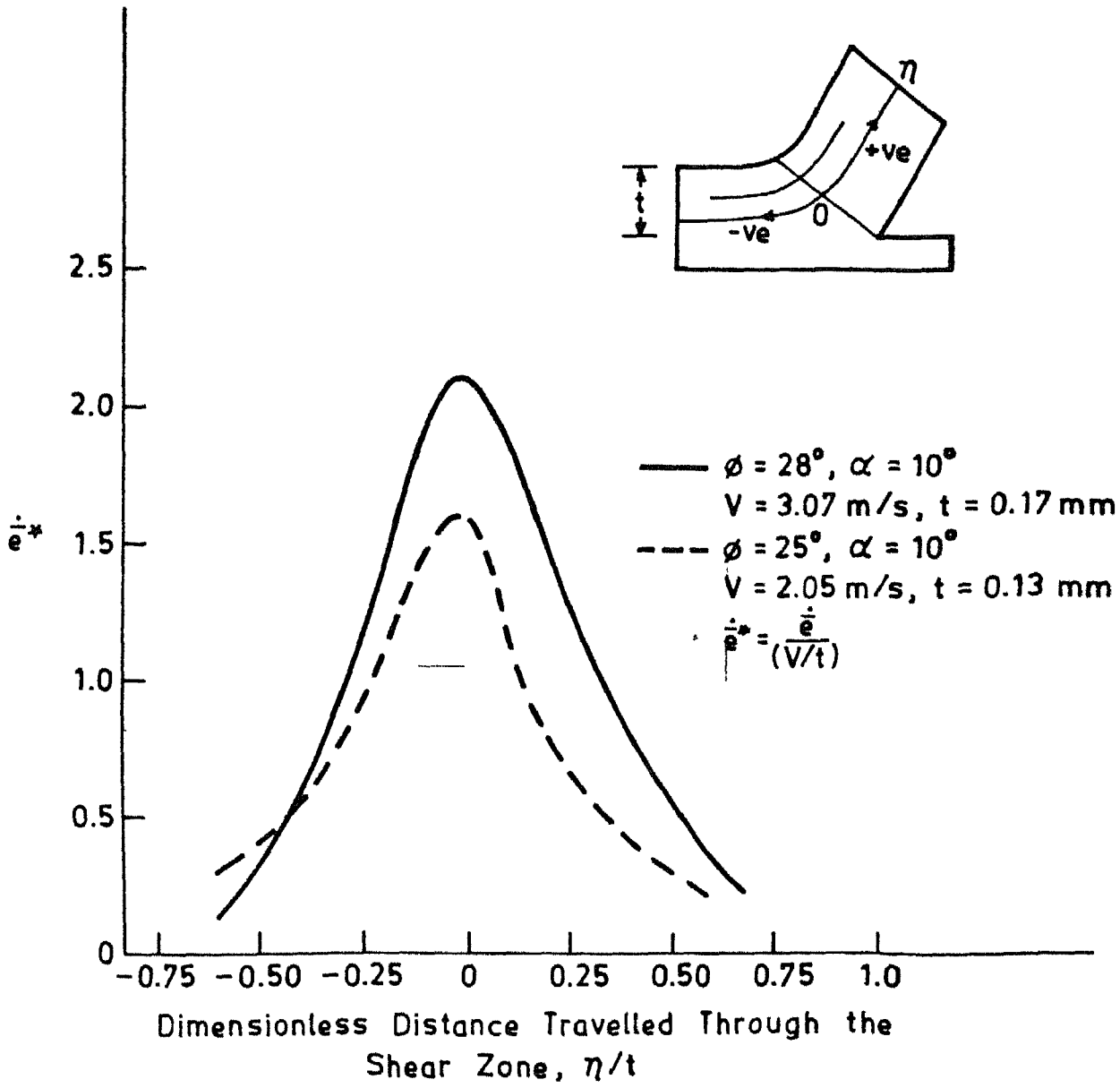

Fig. 4.9. Variation of Dimensionless Strain Rate Across the Shear Zone.

CHAPTER -V

CONCLUSION AND SUGGESTIONS FOR FUTURE WORK

CONCLUSION :

From the results obtained in the present work, the following conclusions can be drawn:

(i) Using the incompressible, non-Newtonian fluid flow for describing the plastic deformation during metal cutting, the primary shear deformation zone can be calculated reasonably accurately.

(ii) A cut off value of 3% of the maximum shear strain rate invariant can be used for approximately demarcating the primary shear zone.

(iii) FEM can be used for solving the velocity and strain rate distribution in the primary shear zone during cutting. It is recommended that Penalty Formulation used (which elliminates the pressure variable) for solving the flow equation. Since inclusion of pressure leads to serious numerical difficulty.

SUGGESTIONS FOR FUTURE WORK :

1. The effects of temperature on plastic flow properties in energy equation and flow equation must be considered.
2. The analysis can be generalised for oblique cutting using three-dimensional formulation.
3. Different type of viscosity equations can be tried for

REFERENCES

1. Merchant, M.E., "Mechanics of Metal Cutting Process ", Pt. I & II, J. Appl. Phys., Vol. 16, 1945, p. 267.

2. Piispanen, V., "Theory of Formation of Metal Chips ", J. Appl. Phys., Vol. 19, 1948, p. 876.

3. Palmer, W.B. and Oxley, P.L.B., "The Mechanics of Orthogonal Machining ", Proc. Instn. of Mech. Engrs, vol. 173, 1959, p. 24.

4. Okushima, K. and Hitomi, K., "On cutting Mechanism of Soft Metals", Trans. Japan Soc. Mech. Engg., Vol. 23, No. 134, 1957, p. 674.

5. Kececioglu, D., "Shear-Strain Rate in Metal Cutting and its effect on Shear Flow Stress ", Trans. Am. Soc. Mech. Engrs., vol. 80, 1958, p.158.

6. Stevenson, M.G. and Oxley, P.L.B., "An Experimental Investigation of the Influence of Speed and Scale on the Strain Rate in a zone of Intense Plastic Deformation ", Proc. Instn. Mech. Engrs, vol. 184, Pt.1, No.31, 1969-70, p.56

7. Black, J.T., "Flow stress Model in Metal cutting ", ASME, J. of Engg. Industry, vol. 95, No.4, 1973, p. 898.

8. Von-Turkovich, B.F., "Deformation Mechanics during Adiabatic Shear ", Proc. II North American Metal Working Res. Conference, Maidson, Wisconsin, 1974, p. 862.

9. Culver, R.S., "Thermal Instability Strain in Dynamic Plastic Defomation- Metallurgical effects at high Strain Rate ", Eds. Plenum Press, Newyork, 1973, p. 519.

10. Bishop, J.P.N., "An Approximated Method for determining the Temperature reached in a Steady State Motion Problem of Plane Strain ", J. Mech. Appl. Math., vol. 9, 1956, p.236.

11. Zienkiewicz, O.C., Jain, P.C and Onate, E., "Flow of Solids during Forming the Extrusion, some Aspect of Numerical Solution", Int. J. Solids Struct., vol. 14, 1978, p. 15.

12. Metirano, R.E. and Gills, P.P., "Viscoplasticity techniques for determining velocity and strain rate fields during extrusion, J. Strain Anal, Vol. 10, No.3,1975, p. 180.

13. Cook, N.H., "Manufacturing Analysis ", Addision Wesley Publication Co., Reading, Mass, 1976.

14. Zienkiewicz, O.C., Onate E. and Heinrichs, "A General Formulation for coupled Thermal Flow of Metals using Finite Element ", Int. J. Nimw Meth. in Engg., Vol. 17, 1981, p. 1497.

15. Zienkiewicz, O.C., The Finite Element Method in Engineering Science, McGraw Hill, 1977)

16. Oslon, M.D., "Variational Finite Element Methods for Two-dimensional and Axisymmetric Navier-Stokes Equations ", Finite Element in fluids, vol. 1, Viscous Flow and Hydro-dynamics, (Ed.) Gallagher R.H. et.al., John Willey, LONDON,

17. Taylor, C. and Hood, P., "A Numerical Solution of the Navier-Stokes Equations using the Finite Element Technique, Computers and Fluids, vol. 1, 1973, p. 73.

18. Henrich, J.C., Marshall, R.S. and Zienkiewicz, O.C., "Penalty function solution of coupled convective and conductive heat transfer ", Proc. Int. Conf. on Numerical Methods in Laminar and Turbulent Flow, Swanable, 1978.

19. Yamda, Y., Ito, K. and Ykouchi, Y., "Finite Element Analysis of steady fluids and Metal Flow ", Flow Symposium, 1974.

20. IRons, B.M., "A frontal solution program for finite element analysis ", Int. J. Num. Meth. in Engg. vol. 2, 1970, p.s.

21. Von-Turkovich, B. and Micheletti, G.F., " Flow Zone Models in Metal cutting ", 9th Int. M.T.D.R. Conf., Univ. of Birmingham, 1968.

22. Nakayama, K., "Studies on the Mechanism of Metal Cutting ", Bull. of the Faculty of Engg., Yokohama Univ. Yokohama, Japan, Vol. 8, 1959.

23. Jain, V.K., and Pandey, P.C., "An Analytical Approach to the Deformation of Mean width of Primary shear Deformation Zone (PSDZ) in Orthogonal Machining ", Proceeding of the 4th Int. Conf. on Prod. Engg., Tokyo, 1980.